A CLOUD CHAMBER STUDY OF

ANOMALOUS θ^{o} PARTICLES

Thesis by

John Amos Kadyk

In Partial Fulfillment of the Requirements

For the Degree of

Doctor of Philosophy

California Institute of Technology

Pasadena, California

1957

Acknowledgments

For his interest, encouragement, numerous suggestions, and general supervision of this thesis, I am very much indebted to Dr. C. D. Anderson, and wish to express my thanks to him.

Throughout the analysis, the discussions with Dr. G. H. Trilling and Dr. R. B. Leighton have been invaluable in forming an accurate and complete understanding of the results. Their interest and suggestions are very much appreciated, both in regard to the analysis, and in preparing the publication of the results. I wish to express my gratitude to them. Many thanks also go to Dr. E. W. Cowan under whose direction my work on anomalous θ^{o} particles began, and who has made many helpful suggestions in regard to the work and the publication based upon it. Dr. Cowan has also contributed several events of excellent quality from the 21" magnet cloud chamber, designed and operated by him.

Mr. Gerry Neugebauer has been of great help through his active interest in this analysis, and in the scanning of films, where he has discovered events of exceptional interest. Dr. C. A. Rouse has contributed an event of particularly great interest, which was obtained during an experiment conducted by him. Mr. Robert Luttermoser has also been very helpful through his interest in the analysis, and by his work in scanning. My thanks go to all these people, who have contributed in an essential way to this investigation.

ABSTRACT

Eighteen anomalous θ^o, (θ^o_{anom}), decay events observed in the magnet cloud chambers have been analyzed. Some of the major problems involved in the analysis are discussed and the methods used to resolve them are described. The results indicate that θ^o_{anom} decays involve 3 or more secondary particles, and probably arise from a K^o meson having approximately the mass of all other known K particles, viz. 966 m_e. Many of the decays are found to be dynamically inconsistent with the $\tau^o \longrightarrow \pi^+ + \pi^- + \pi^o$ scheme, but most are consistent with the decay processes: $\theta^o_{anom} \longrightarrow \pi^+ + \pi^- + \gamma$, $\pi^\pm + \mu^\mp + \nu$, and $\pi^\pm + e^\mp + \nu$. However, at least one event is inconsistent with each decay scheme. From the locations of the decays in the cloud chamber, the lifetime is found to be significantly longer than that of the normal θ^o particle, called here the $\theta^o_{\pi 2}$ particle. Other differences in the behavior of the θ^o_{anom} and $\theta^o_{\pi 2}$ particles were also observed in the (a) momentum distributions, (b) origin locations, (c) relative numbers of θ^o_{anom} and $\theta^o_{\pi 2}$ particles traveling upward, and (d) the types of V particles produced in association with the θ^o_{anom} and $\theta^o_{\pi 2}$. It is concluded that not all the θ^o_{anom} decays can result from alternate decay modes of the $\theta^o_{\pi 2}$. Moreover many decays can be neither τ^o decays nor alternate decays of the $\theta^o_{\pi 2}$.

The characteristics of the θ^o_2 particle proposed by Gell-Mann and Pais are consistent with those of the θ^o_{anom}

particle, with the possible exception of the observed types of associations. An estimate was made of the relative number of θ^o_{anom} to $\theta^o_{\pi 2}$ particles observed to decay in the cloud chamber. If all θ^o_{anom} decays are assumed to arise from decays of the θ^o_2 particle, then a lower limit for the θ^o_2 lifetime is found to be about 10^{-9} sec.

TABLE OF CONTENTS

I. INTRODUCTION

Previous to 1953, the only known V^o particles consisted of the Λ^o,[1] a hyperon* decaying by the scheme

$$\Lambda^o \longrightarrow p + \pi^- + 37 \text{ Mev} \qquad (1)$$

and the $\theta^o_{\pi 2}$,* a K meson which has the decay mode[1]

$$\theta^o_{\pi 2} \longrightarrow \pi^+ + \pi^- + 214 \text{ Mev} \qquad (2)$$

Each of these V^o particles* decays into only two secondary particles. In addition, there were known to exist several charged hyperons and K mesons,* most of which decayed into only two secondaries, but a few of which decayed into at least 3 secondaries, e.g.[1]

$$\tau^+ \longrightarrow \pi^+ + \pi^- + \pi^+ + 75 \text{ Mev} \qquad (3)$$

The first strong evidence that V^o particles do not always decay by a two-body mode was presented by Van Lint,[2] Thompson,[3] and the Princeton group.[4] They found among the many V^o decays, a few cases in which the positive secondary was clearly not a proton, and yet the Q value calculated for the $\theta^o_{\pi 2}$ decay was markedly lower than 214 Mev.[5] More-

---

* See p. 2 for terminology.

Terminology for Fundamental Particles

1. Classification According to Rest Mass

   a. Hyperon: an elementary particle heavier than a neutron, always decaying finally into a neutron or proton.

   b. Baryon: a hyperon, neutron or proton.

   c. K Meson: any known particle having a mass intermediate to the π meson and proton masses. All presently known K mesons have a mass of about 966 m_e.

   d. L Meson: a light meson, i.e. a π or μ meson.

2. V Particles

   "V particle" is a description which includes all fundamental particles which are observed to decay in cloud chambers, other than π or μ mesons.

3. Sign of Charge

   The sign of charge is usually denoted by a superscript, e.g. V^+, V^-, and K^o for charged V particles, and a neutral K particle.

4. $\theta^o_{\pi 2}$ is used to denote the particle from which the $\pi^+ + \pi^-$ decay arises, instead of θ^o as previously used. This convention is in accord with the present notation for charged K mesons. Correspondingly, θ^o_{anom} denotes the particle from which the anomalous θ^o decays arise.

over, in most of the cases in which an origin was observed, the origin did not lie in the plane of decay formed by the two charged secondaries. Since the secondaries could sometimes be identified as L mesons,* and no evidence existed that any secondary was heavier than an L meson, the new V^o was presumed to be a K^o meson, and was called an "anomalous θ^o" (θ^o_{anom}) particle.

It is reasonable to argue that these events were not new types of decays, but were merely cases in which there existed extraordinarily large distortions of the tracks, leading to erroneous Q values, and that the origins were incorrectly identified, leading to apparent non-coplanarity. However, this cannot be the explanation of all θ^o_{anom} decays, since some events having the most anomalously low Q values are those which are notably free from any evidence of distortions; furthermore, there appears to be a strong correlation between the apparent Q value and the extent to which the origin is non-coplanar with the decay. These characteristics strongly suggest that the θ^o_{anom} decay involves more than two secondaries, implying the existence of one or more neutral secondaries.

Several possible decay schemes have been proposed to explain the θ^o_{anom} decay. Two early suggestions were that (a) the θ^o_{anom} decay was the neutral counterpart of the decay 3, viz. $\tau^o \longrightarrow \pi^+ + \pi^- + \pi^o$, or (b) that the θ^o_{anom} decay

---

* See p. 2 for terminology.

was a 3-body alternate decay of the $\theta^o_{\pi 2}$ particle.[2] Recently, an explanation has been proposed[6] based upon certain unique properties of the θ^o meson. According to this idea, both the θ^o and its antiparticle, $\overline{\theta}^o$, are particle "mixtures," each exhibiting two distinct lifetimes, and decaying at least half of the time by a 3-body decay mode.

These ideas and others are investigated in the present analysis in an effort to describe the θ^o_{anom} particle and its decay modes, and this leads to the first evidence for the existence of a V^o particle other than the Λ^o and $\theta^o_{\pi 2}$[7].

LIST OF SYMBOLS

B = magnetic field strength in MKS units (webers/meter^2).

L = chord length of arc of a circle.

$\underline{P}\pm, I\pm, M\pm$ = the momentum, ionization, and mass, respectively of the positive or negative secondary.

$\underline{P}$ = vector sum of the momenta of charged secondaries as measured in the laboratory system.

$\underline{P}^*$ = vector sum of the momenta of charged secondaries as measured in the center-of-mass system. P^* is also the magnitude of momentum of the neutral secondary or secondaries in this system.

$P_\perp$ = the component of $\underline{P}$ perpendicular to the line of flight of the θ^o_{anom} particle. $P_\perp$ is also equal to the component of momentum transverse to the θ^o_{anom} line of flight of any neutral secondary or secondaries, and is the same in both the laboratory and center-of-mass systems.

P_o, M_o = the momentum and mass of the parent particle, which undergoes decay.

$Q(1,2)$ = the Q value computed on the assumption of a two-body decay into the charged secondaries 1 and 2.

m_1, m_2 = masses of charged secondary particles.

m_3 = mass of neutral secondary particle

m_e = mass of electron = .511 Mev.

p = momentum of any particle observed in cloud chamber.

p_{max} = maximum detectable momentum of particle observed in cloud chamber.

S = sagitta distance for arc of a circle.

S_M, S_D, S_S = assigned measurement, distortion and scattering errors in S, respectively, corresponding approximately to one standard deviation.

e = the total relative or fractional error in S.

e_M, e_D, e_S = the relative or fractional errors in S corresponding to S_M, S_D, S_S, respectively.

$$\alpha = \frac{P_+^2 - P_-^2}{P^2}$$

$$\beta = \frac{v}{c} = \text{particle velocity in units of light velocity.}$$

$$\gamma = \frac{1}{\sqrt{1 - \beta^2}}$$

$$\gamma\beta = \frac{P_o}{M_o} = \frac{\beta}{\sqrt{1 - \beta^2}}$$

δ = the angle between the assumed line of flight of the Θ^o_{anom} particle and the plane determined by the tracks of the charged secondaries.

Θ = the included angle between the V^o charged secondaries.

ρ = radius of curvature, in centimeters.

ϕ, ϕ^* = the angles between the Θ^o_{anom} line of flight and $\underline{P}$ or $\underline{P}^*$, respectively.

II. ANALYSIS OF EVENTS

A. Problems of Analysis.

The analysis of θ^{o}_{anom} events, which occur only rarely among V^{o} decays, requires a somewhat different approach than the analysis of the more abundant decays, such as Λ^{o} and $\theta^{o}_{\pi 2}$ decays. It is relatively easy to select Λ^{o} or $\theta^{o}_{\pi 2}$ decays with only a small contamination, since the θ^{o}_{anom} decays are rare. However, in seeking to analyze the θ^{o}_{anom} decays, the contamination now consists of the more abundant $\theta^{o}_{\pi 2}$ and Λ^{o} decays, and so a rigorous method of selection must be employed to insure that the contamination is small. Moreover, the problem is made doubly difficult by setting a high standard for selection of events, since some θ^{o}_{anom} events of poorer quality which would nevertheless be useful, are certainly rejected along with the contamination. This further reduces the number of events in the desired sample, and increases the statistical error.

The nature of the 3-body decay of θ^{o}_{anom} particle is also very troublesome in many respects. Because the momentum of the neutral secondary is unknown, the direction of motion of the θ^{o}_{anom} particle is uncertain when no origin is observed. If several possible origins are closely grouped, it is usually impossible to identify the correct origin. Even with an unambiguous origin present, it is usually not possible to compute a unique value for the momentum of the θ^{o}_{anom} particle, P_{o}, because the component of

momentum of the neutral secondary along the θ^o_{anom} line of flight cannot, in general, be determined. The calculation of P_o will be described more fully in part V on Lifetime Analysis.

In order to discriminate between θ^o_{anom} and $\theta^o_{\pi 2}$ decays it is usually necessary to rely on the Q value computed for the $\theta^o_{\pi 2}$ decay. As a consequence of the errors of measurement, it is usually impossible to distinguish between a $\theta^o_{\pi 2}$ decay and a θ^o_{anom} decay having an apparent Q value over 100 Mev.

B. Selection Criteria

In order to select as objectively as possible the θ^o_{anom} events to be used for the analyses, it seemed that standard selection criteria should be established which must be rigorously fulfilled by each acceptable event. For this purpose certain error formulae were developed by which the measurement errors could be reliably and quickly computed. These formulae will be discussed in the following section.

The selection criteria may be divided into two distinct groups, according to their function. Starting with the complete sample of all V^o events observed in the cloud chambers, the criteria in group A are designed to eliminate all Λ^o events, while keeping as many $\theta^o_{\pi 2}$ and θ^o_{anom} events as possible. From the events which remain, the θ^o_{anom} decays

are selected by the requirements of group B. In order to be acceptable as a θ^{o}_{anom} event, each V^{o} event must satisfy at least one requirement both in group A and in group B.

Group A

1. The ionization and momentum of the positive secondary restrict its mass to be less than the proton mass.
2. The quantity P-sinθ exceeds 118 Mev/c by an amount outside experimental error.(8)
3. $\alpha < 0$ for an event for which P > 300 Mev/c(9)

No ordinary Λ^{o} decay event can satisfy any of these criteria. In addition, it was required that no event could be interpreted as a charged V, π-μ, or μ-e decay,* or a scattering. There were found to be 256 events satisfying these criteria.

Group B

1. $Q(\pi^{+},\pi^{-}) < 214$ Mev(5) by at least 2 standard deviations.
2. For events having a well-defined origin in the material immediately adjacent to the chamber in which the decay occurs, the origin lies outside the plane of decay by more than two standard deviations.

---

* One event (69328) could be a decay in flight of a μ^{+} traveling upward, but this interpretation seems very unlikely on the basis of the long lifetime of the μ^{+}.

Eighteen events were found to satisfy the above criteria of group B and qualified as θ^{o}_{anom} events; all except one of these qualified under requirement 1.

C. Error Formulae*

The selection or rejection of events to be used in the sample of θ^{o}_{anom} decays depends to a very large degree upon the computed value of $Q(\pi^+,\pi^-)$, which in turn depends upon the measurements made upon the V^o decay. The basic measurements made upon a V^o decay event are P_+, P_-, and θ.(10) Quantities that are derived from these measurements, such as $Q(\pi^+,\pi^-)$ and P_o, normally are little affected by an error in θ as compared to the effect of errors in P_+ and P_-. This is because measurements of purely geometric quantities, such as θ, can be made very accurately with the present reprojection system. Therefore, it is important to establish a good method of assigning momentum errors.

The determination of momentum is based upon the formula for curvature of a track perpendicular to a uniform magnetic field,

$$p(Mev/c) = 3B\rho \qquad (4)$$

Appropriate corrections, which are usually small, are made for the known inhomogeneity of the field, and for the effect of conical projection in the photographic process.(11) Since the measurement of a chord length and its sagitta

---

* See Appendix A for a more detailed treatment of the formulae discussed in this section.

uniquely determine the circle's radius by the relation

$$\rho = \frac{L^2}{8s} + \frac{s}{2} \tag{5}$$

the momentum can be easily computed from L and S. This is done by tracing the image formed by an anisotropic projector,[12] which magnifies the sagitta 10 times more than the track length. By this procedure, relatively little error is introduced in the measurement process, and the measurement can be made quickly and conveniently.

1. Measurement Error

A constant random error, S_M, has been assumed to exist in the measurement of the sagitta. S_M has been determined empirically by selecting several tracks of various momenta and plotting for each the distribution of many measurements made on the track. A value for S_M of 1/5 of a track width, or $S \simeq 0.02$ cm, seems to represent about 1 standard deviation. The fractional measurement error in S is therefore given by

$$e_M = \frac{S_M}{S} \tag{6}$$

2. Distortion Error

The errors arising from convection currents within the chamber are difficult to ascertain to a high degree of reliability, because such distortions change frequently in a more or less unpredictable manner. One cannot accurately

assign a distortion error based upon the general appearance of tracks in a single photograph, for frequently there is no way to distinguish between slightly distorted and badly distorted tracks. Furthermore, the absence of distortion in one part of the chamber is not strong evidence that distortions are not present elsewhere in the chamber. Nevertheless, it was felt that a formula could be found which would give a reliable estimate of distortion errors in a statistical sense.

The formula for distortion error was developed by finding first a reasonable relationship between S_D, P_{max}, and L. For moderately large L, the maximum detectable momentum, P_{max}, is determined almost entirely by distortion error. Furthermore, it is known from experience that P_{max} increases with L. By combining equations 4 and 5 we find

$$P_{max} \simeq 3B \frac{L^2}{8S_D} \qquad (7)$$

Evidently, S_D cannot be proportional to L^2, or P_{max} would not depend on L. Furthermore, S_D cannot be independent of L, since S_D must vanish for small L. Since S_D clearly increases with L, the simplest possible assumption is that S_D is proportional to L, given by

$$S_D = 0.036\left(\frac{L}{20}\right) \text{ cm.}\ ;\ e_D = \frac{S_D}{S} \qquad (8)$$

This formula has been normalized to give P_{max} = 3.3 Bev/c for L = 20 cm, which is observed experimentally.[11] This relation has been checked for internal consistency with a group of about 50 $\theta^0_{\pi 2}$ decays, and the result indicates that

the assigned distortion error is at least as large as a standard deviation.

3. Scattering Error

The scattering error has been calculated from a formula based upon an analysis by Bethe.[13]

$$\frac{|\Delta\rho|}{\rho} = (16.5\times10^{-4})\frac{Z}{B}\frac{1}{\beta}\sqrt{\frac{2NA}{L}} \qquad (9)$$

where: N = $\frac{\text{moles}}{\text{cm}^3}$ of gas in chamber

Z = Atomic number of gas

A = dimensionless quantity near unity, and slowly varying.

For most cases, $\frac{|\Delta\rho|}{\rho} < 10\%$, and the following relation is approximately true:

$$e_s = \frac{S_s}{S} = \frac{|\Delta(\frac{1}{\rho})|}{\frac{1}{\rho}} \simeq \frac{|\Delta\rho|}{\rho} \qquad (10)$$

This permits e_S to be combined quadratically with e_M and e_D, which are directly proportional to the error in sagitta, and the result is the total relative error in S:

$$e = \sqrt{e_M^2 + e_D^2 + e_S^2} \qquad (11)$$

The errors e_M, e_D, and e_S are readily calculated using the equations 6, 8, and 10. The total error e is proportional to $\frac{1}{\rho}$ (except for very small ρ), and since the errors in

S are expected to be distributed symmetrically about S the errors in p are not symmetric, unless e is small. The positive error in p is always as large or larger than the negative error, the errors being given by

$$\pm \Delta p = \frac{p}{\left(\frac{1}{e}\right) \mp 1} \tag{12}$$

The errors in Q value were calculated from the relations[10]

$$\frac{\partial Q}{\partial P_+} = \frac{\frac{P_+}{E_+} E_- - P_- \cos\theta}{m_+ + m_- + Q} \; ; \quad \frac{\partial Q}{\partial P_-} = \frac{\frac{P_-}{E_-} E_+ - P_+ \cos\theta}{m_+ + m_- + Q} \tag{13}$$

$$\pm \Delta Q_+ = \frac{\partial Q}{\partial P_+} (\pm \Delta P_+), \; \pm \Delta Q_- = \frac{\partial Q}{\partial P_-} (\pm \Delta P_-), \; \pm \Delta Q = \sqrt{(\pm \Delta Q_+)^2 + (\pm \Delta Q_-)^2} \tag{14}$$

The derivatives were evaluated using the measured values of P_+ and P_-. Only an approximate value for $\pm \Delta Q$ is obtained from relations 13 and 14. This is because Q is a complicated function of P_+ and P_- , and only the first term in the Taylor's series expansion for ΔQ has been used. However, it was found that higher terms in the expansion are sufficiently small that the results are not altered by using the approximate relations 13 and 14. Since the errors in $P_\pm$ are non-symmetric, so also are the errors in ΔQ, as can be seen from relations 14.

III. DATA

A. Tables of Measurements

In table I are listed the results of measurements made upon the secondaries of each θ^{o}_{anom} decay and table II gives some of the principal features of the events.

The ionization estimates in table I are based upon the independent estimates of 3 observers, and are used with the momentum measurements to find mass limits of each secondary particle. It should be noted that in every event the positive secondary is found to be less massive than a proton. Of particular interest are 6 events where one secondary is identified as an L meson, and one event where both secondaries are identified as L mesons. This is the only known case of θ^{o}_{anom} decay into two L mesons. Also of interest is one event having an identified electron secondary.

In table II, the angle of non-coplanarity, δ, and the momentum unbalance, $P_{\perp}$ were calculated only for those events having a clearly defined and unambiguous origin. There are several characteristics of considerable interest in table II: (a) Most origins are markedly non-coplanar, and the degree of non-coplanarity appears to increase as the $Q(\pi^{+},\pi^{-})$ value decreases. (b) 3 θ^{o}_{anom} particles apparently occur in association with other V particles, and (c) 4 θ^{o}_{anom} particles can definitely be identified as traveling in an upward direction. These characteritics will be dis-

Table I. Main features of θ^{o}_{anom} secondaries

Event No.	P_+ (Mev/c)	I_+ (I_{min})	M_+ (m_e)	P_- (Mev/c)	I_- (I_{min})	M_- (m_e)	θ (deg)
			48" Chamber				
04480	105^{+40}_{-23}	<2.0	<320	120^{+15}_{-12}	<1.7	<280	118
19143[a]	250 ± 23	<1.5	<500	88 ± 5	1.6-3.2	170-320	40.7
31855	156 ± 6	<2.0	<400	88 ± 5	1.5-2.5	160-260	21.5
35045	132^{+34}_{-22}	<2.1	<330	330^{+330}_{-110}	<2.0	<1500	25.3
36537	---	<1.5	---	206 ± 12	<1.5	<400	92.9
36894	233 ± 19	<1.2	<310	75^{+22}_{-14}	1.5-3.0	110-330	118
37663	655^{+145}_{-100}	<2.0	<1800	360 ± 35	<2.0	<900	30.7
39522	562^{+320}_{-150}	<2.0	<1800	547^{+180}_{-110}	<2.0	<1700	17.2
45766	192 ± 12	<1.5	<350	30 ± 4	6.5-10.0	150-250	46.2
47202	101 ± 6	1.5-3.0	185-350	94 ± 6	1.5-3.0	170-320	61.8
56500	51^{+10}_{-7}	3.0-6.0	150-340	89^{+20}_{-14}	<2.6	<380	65.2
56791	355^{+80}_{-55}	<1.5	<800	120^{+54}_{-30}	2.0-4.0	150-500	77.6
57680	107 ± 11	<1.5	<300	610^{+250}_{-150}	<1.5	<1000	19.9
60134	226 ± 9	<2.0	<550	389^{+76}_{-55}	<1.5	<900	65.8
69328	$11.9\pm.9$	<1.5	<12	200^{+36}_{-27}	<1.5	<380	46.1
			21" Chamber				
10475	594 ± 57	<2.0	<1500	1247^{+460}_{-330}	<2.0	<3000	16.0
12590[a]	595^{+170}_{-110}	<2.0	<1500	243^{+50}_{-36}	<2.0	<600	34.2
20923	554 ± 34	<2.0	<1400	198^{+50}_{-33}	<1.6	<400	52.2

Table I - continued

[a] Given are the results of remeasurement of Events 19143 and 12590 which were published in reference 2. Event 15329 upon remeasurement seems to be somewhat dubious and has been omitted from this sample.

Table II. Decay dynamics of θ^0_{anom} events

Event No.	$Q(\pi^+,\pi^-)$ (Mev)	δ (deg)	$P_\perp$ (Mev/c)	Comments
		48" Chamber		
04480	60^{+21}_{-12}	---	---	
19143	35 ± 2.5	29.5 ± 4	181 ± 30	Probable $\theta^0_{\pi 2}$ association
31855	10.3 ± 1	33.5 ± 4	175 ± 18	Probable K^+ association
35045	32^{+58}_{-20}	11.7 ± 2	107^{+100}_{-34}	
36537	---	19.4 ± 9	~ 150	Travels upward
36894	96 ± 12	---	---	Travels upward[b]
37663	112^{+26}_{-18}	2.4 ± 4	46^{+70}_{-46}	Probable V^+ association
39522	45^{+16}_{-12}	1.6 ± 2	90^{+80}_{-47}	
45766	34 ± 4	---	---	
47202	17 ± 5	16.4 ± 1	108 ± 5	Travels upward
56500	10^{+4}_{-3}	---	---	
56791	123^{+37}_{-24}	12.7 ± 3	89^{+34}_{-24}	Travels upward
57680	90^{+48}_{-30}	4.4 ± 2	73^{+35}_{-26}	
60134	152^{+28}_{-21}	---	---	
69328	$8.3\pm.7$[a]	3.3 ± 2	21 ± 14	Λ^0 decay also present probably not associated
		21" Chamber		
10475	98^{+42}_{-25}	0.6 ± 5	49^{+22}_{-47}	
12590	92^{+33}_{-21}	3.5 ± 4	58 ± 50	
20923	147^{+18}_{-14}	---	---	

Table II - continued

[a] The value given is $Q(\pi^-, e^+)$, since the positive secondary is identified as an electron.

[b] Based on decay dynamics, since no origin is observed. A θ^o_{anom} mass of 966 m_e is assumed.

cussed later in more detail.

B. Events of Particular Interest

Shown in figure 1 through figure 4 are several events of particular interest. Figures 1 and 2 show a θ^{o}_{anom} decay which is manifestly out of line with its only apparent origin, and is also apparently associated with a K^{+} particle. The decay in figure 3 arises from an upward moving θ^{o}_{anom} particle, and is clearly out of line with the origin.* This decay event is the only known θ^{o}_{anom} decay in which both charged secondaries are identified as L mesons, and is one of the few events consistent with the $\tau^{o} \rightarrow \pi^{+} + \pi^{-} + \pi^{o}$ decay.

The negative secondary in figure 4 is very slow, and ionizes quite heavily. It appears to stop in the front glass of the cloud chamber. Closely coincident with the end of the heavy track there appears a lightly ionizing negative track, which is identified as an electron. This presumably indicates that the secondary is a μ^{-} meson, since a π^{-} is strongly absorbed in solids and does not decay. However, the secondary is so slow that it could have stopped in the argon gas before reaching the front glass. There is insufficient knowledge available at present to determine the probability of π^{-} absorption in argon gas, but there seems to be reason to believe that an appreciable chance exists of π^{-} decay; if this is so, a $\pi^{-} - \mu^{-}$ decay

---

* This event was obtained during an experiment conducted by Dr. C. A. Rouse, and is used with his permission.

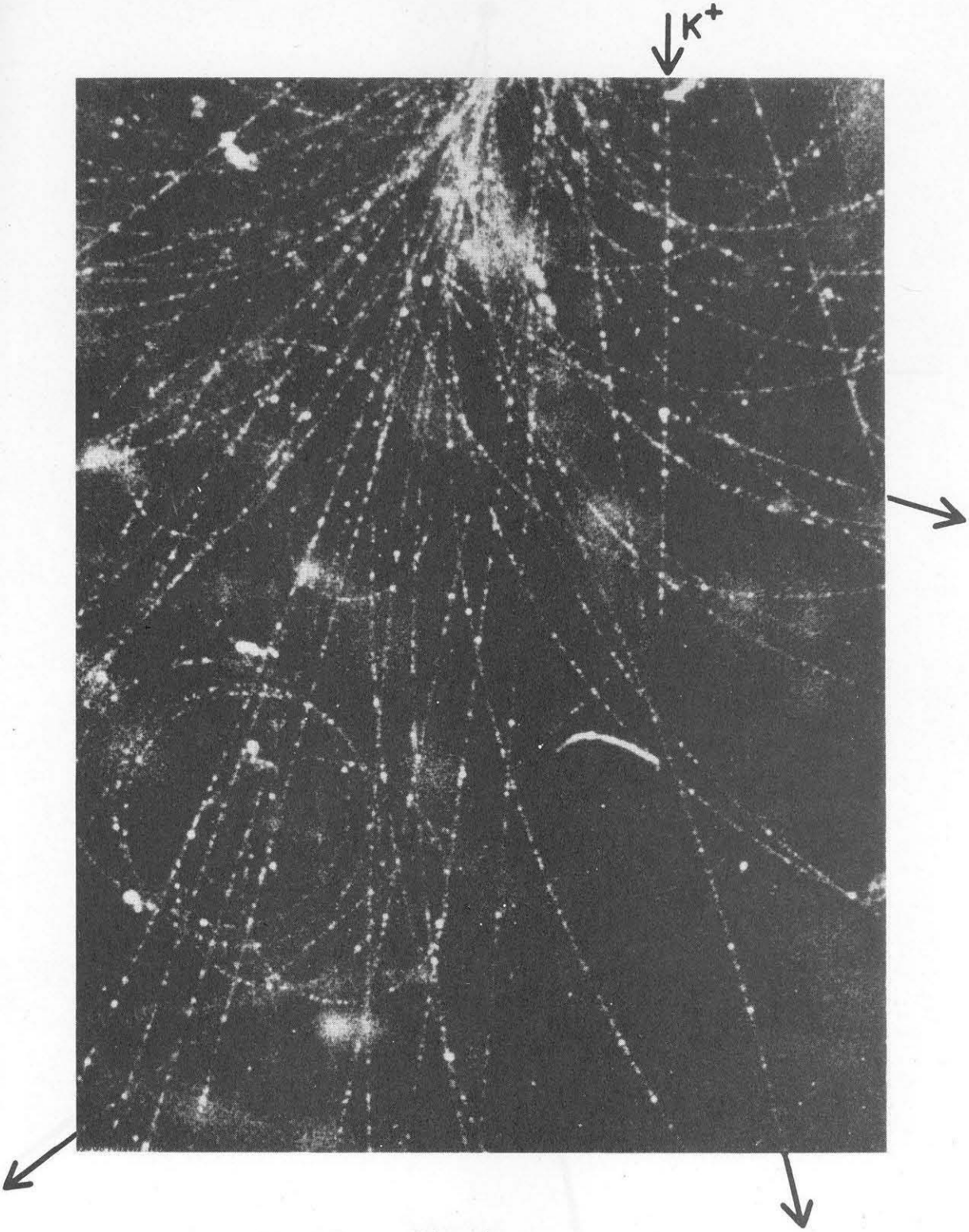

Fig. 1

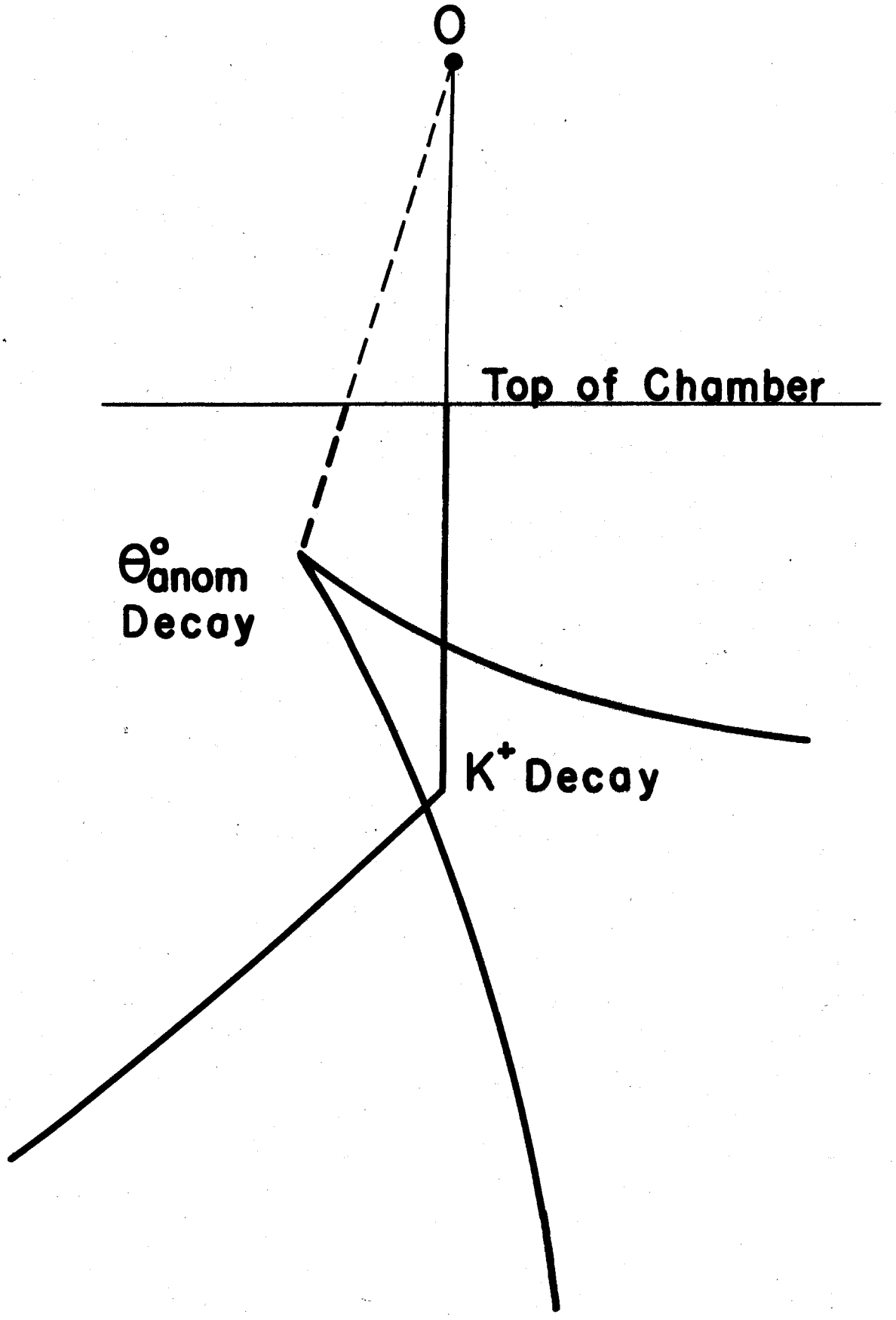

Fig. 2

• Origin

Fig. 3

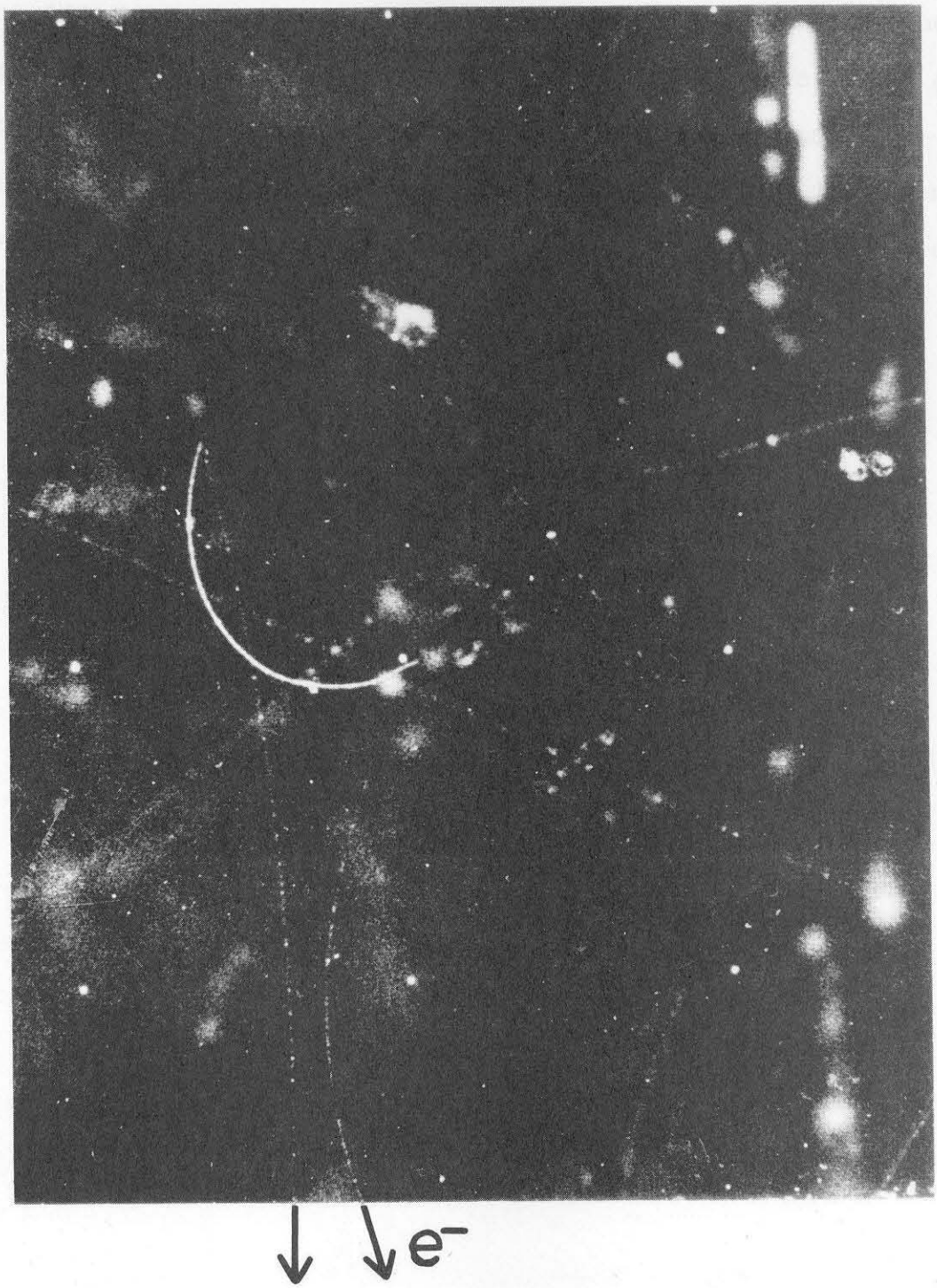

Fig. 4

may have occurred unobserved in the poorly illuminated region near the front glass, and the μ^-, stopping in the glass, would have decayed into the observed electron. Although it is impossible to say with certainty that the negative secondary is a μ^-, this identification is strongly suggested. Furthermore, there is good reason to believe such a decay scheme exists by analogy with the recently established decay:(14)

$$K^+_{\mu 3} \longrightarrow \mu^+ + \pi^0 + \nu$$

IV. DYNAMICAL ANALYSIS

A. Methods of Analysis

The analysis of the θ^o_{anom} events is done in two fundamentally different ways. (1) The decay products and dynamics were analyzed to determine whether the decays are compatible with certain suggested schemes, and (2) the lifetime is found and other properties of the θ^o_{anom} particle are investigated to determine if the θ^o_{anom} decay is an alternate decay of the $\theta^o_{\pi 2}$ particle, or if not, what is the nature of the particle. In this section, the investigation of decay products and dynamics will be discussed.

One method of determining decay modes is by identification of the secondary masses, using the estimated ionizations and measured momenta. Unfortunately, the secondaries are normally too fast to ionize heavily and one usually cannot distinguish between electrons, π and μ mesons among the decay products.

A more fruitful approach makes use of the decay dynamics by plotting $P_\perp$ vs $Q(1,2)$ for each event having an origin. This is done for various assumed decay schemes having secondaries 1 and 2, and depends on the fact that different Q values exist for different schemes assuming that all θ^o_{anom} decays arise from parent particles of the same mass. Consequently, in the center-of-mass system

(C.M. system) the secondary particles are emitted with different average momenta for different schemes. Figure 5 illustrates the decay processes as seen in the C. M. system and the laboratory system. Assuming all θ^{o}_{anom} decays arise from a particle of mass M_o, then the following relation exists between the Q(1,2) value and P* for each decay process,* for a 3-body decay:

$$P^* = \sqrt{\left\{\frac{M_o^2 + m_3^2 - [m_1 + m_2 + Q(1,2)]^2}{2M_o}\right\}^2 - m_3^2} \qquad (15)$$

This reduces to a simpler form when $m_3 = 0$:

$$P^* = \frac{M_o^2 - [m_1 + m_2 + Q(1,2)]^2}{2M_o} = \frac{M_o^2 - M^2}{2M_o} \qquad (16)$$

Since the component of momentum transverse to the θ^{o}_{anom} line of flight is the same in both the laboratory and C.M. systems,

$$P_\perp = P_\perp^* = P^* \sin \phi^*$$

Hence P* is an upper limit on $P_\perp$, which can be measured. Furthermore, if the decay is isotropic in the C.M. system (which is expected if these are K^o particles of zero spin, as some results indicate), then the angular decay distribution is proportional to sin ϕ^*, enhancing the decays with $P_\perp$ close to P*. Thus, most decay points should tend to

---

* See Appendix B.

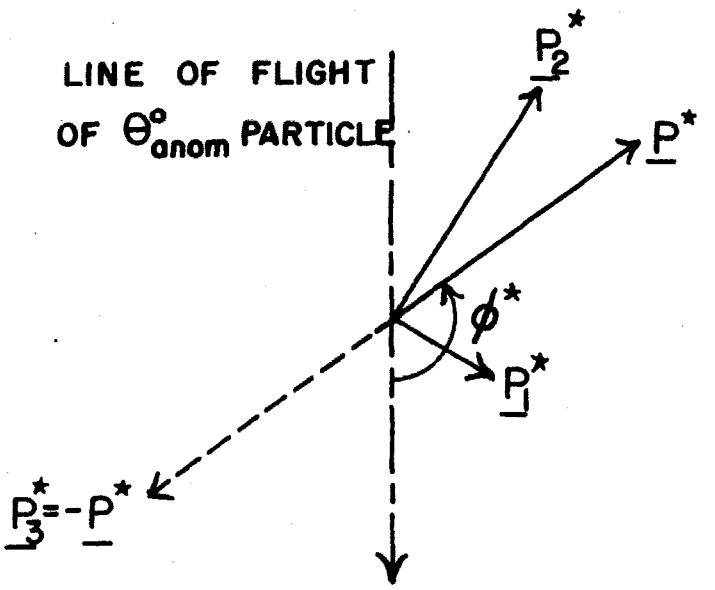

CENTER-OF-MASS SYSTEM

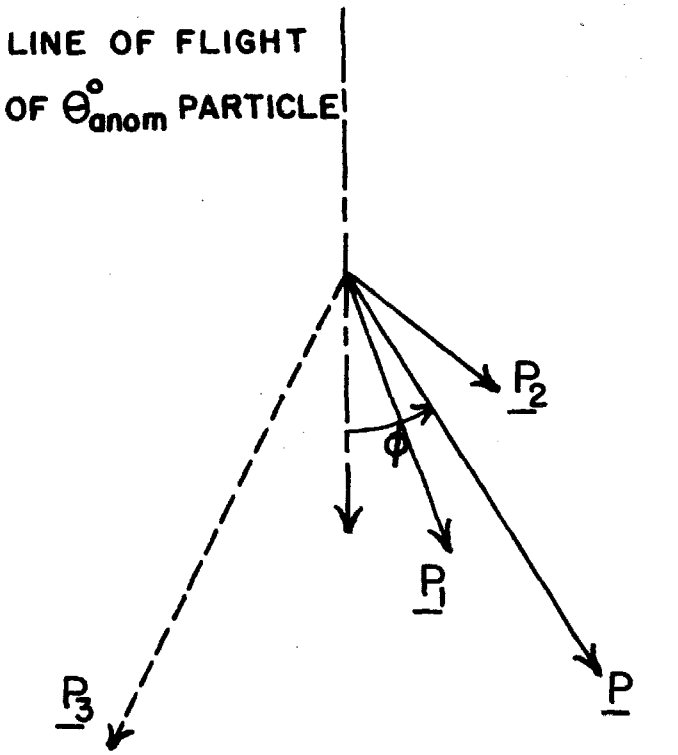

LABORATORY SYSTEM

Figure 5

cluster closely below the curve for P*, giving a sensitive indication of compatibility. This dynamical method will be used here in the discussion of four decay schemes. For this purpose, the mass, M_o, has been chosen equal to that of all presently known K particles, 966 m_e. An additional justification of this choice will be discussed later.

B. Results of Dynamical Analysis

(A) $\theta^o_{anom} \equiv \tau^o \longrightarrow \pi^+ + \pi^- + \pi^o + 80$ Mev

The decay scheme A is the neutral counterpart of the τ^+ and τ^- decay schemes. One θ^o_{anom} event, pictured in figure 3, is best interpreted as an example of this decay on the basis of dynamics and the identification of both secondaries as L mesons. However, there was early evidence that not all decays could be of this type,[2,3] and strong evidence exists from the present data that most decays cannot be of scheme A. There is one event (see table I) which decays into an identified electron secondary. Four other events have $Q(\pi^+,\pi^-)$ values greater than 100 Mev (see table II), and are quite unlikely to be τ^o decays. Additional proof is provided by a study of figure 6, where $P_\perp$ vs. $Q(\pi^+,\pi^-)$ is plotted for 10 events having origins and measurable Q values; curve A gives P* as a function of $Q(\pi^+,\pi^-)$ for the τ^o decay. Of the 10 plotted points, 9 lie outside curve A, and 4 fall outside by 2 or more standard deviations. Altogether there are 8 events clearly incon-

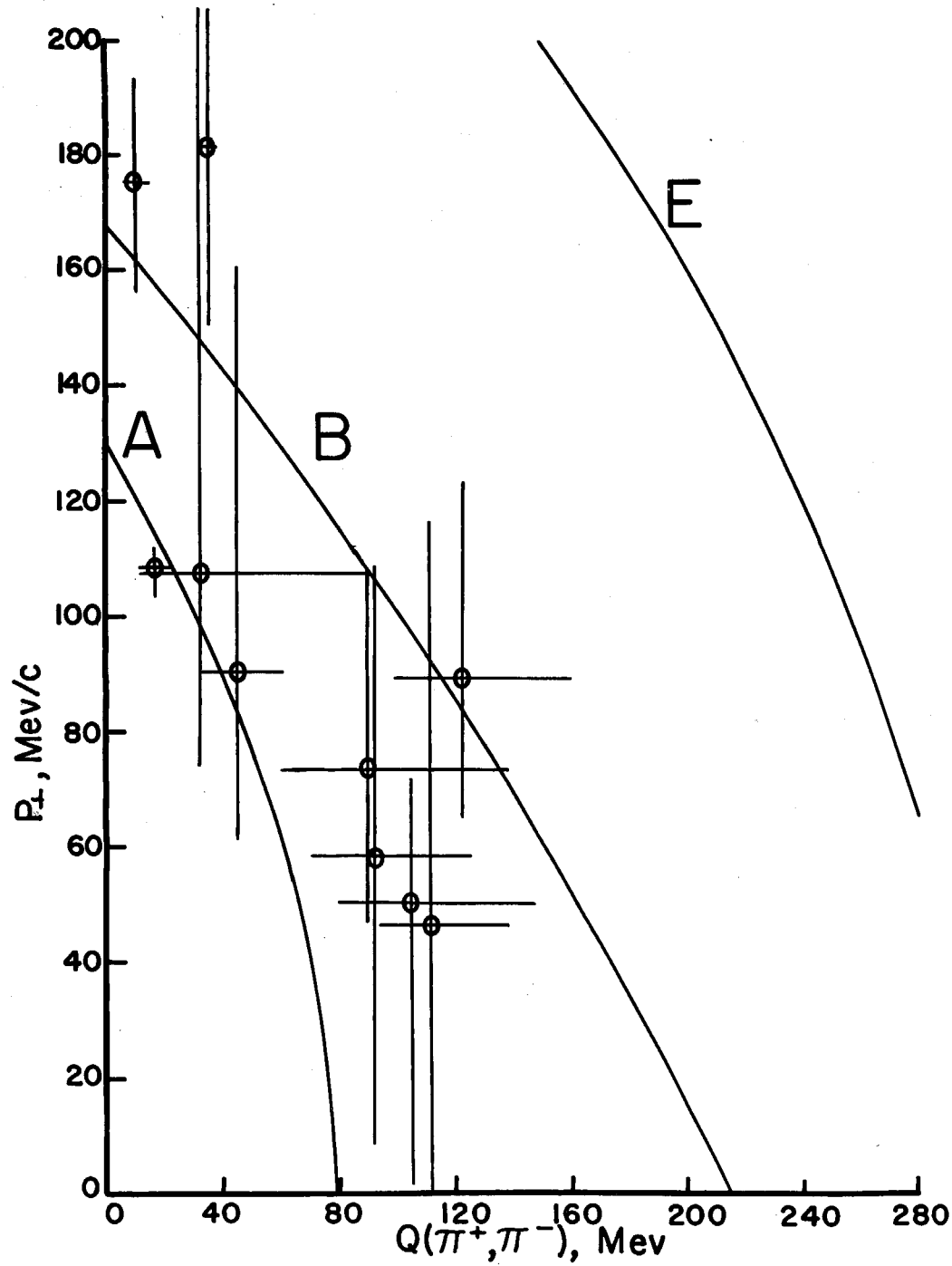
200
180
160
140
120
100
80
60
40
20
0
$P_\perp$, Mev/c
A
B
E
0
40
80
120
160
200
240
280
$Q(\pi^+,\pi^-)$, Mev

Figure 6

sistent with scheme A, and 5 more which probably are not examples of this decay. Thus, most, if not all of the θ^o_{anom} events do not decay by scheme A.

$$(B)\ \theta^o_{anom} \longrightarrow \pi^+ + \pi^- + \gamma + 214\ Mev$$

This decay suggests a radiative decay of a $\theta^o_{\pi 2}$. However, it has been shown[15] that it is exceedingly unlikely that a radiative correction to the $\theta^o_{\pi 2}$ decay could give rise to the low $Q(\pi^+,\pi^-)$ values observed. Perhaps, however, the γ ray may play a more fundamental role in the decay process, and may be on an equal status with the other secondary particles.

Curve B in figure 6 shows P* vs. $Q(\pi^+,\pi^-)$ for scheme B. Although 3 points lie outside curve B, none of these lies as much as two standard deviations from the curve, so that the events, as a group, are not inconsistent with scheme B.

$$(C)\ \theta^o_{anom} \longrightarrow \mu^{\pm} + \pi^{\mp} + \nu + 248\ Mev$$

Evidence for the decay $K^+_{\mu 3} \longrightarrow \mu^+ + \pi^o + \nu$ has been found[14] with the use of emulsions. The scheme C then appears reasonable as the neutral counterpart of the $K^+_{\mu 3}$ decay.

Figure 7 shows the result of the analysis based upon scheme C. Since $Q(\pi,\mu)$ depends only slightly on which charged secondary is the π and which the μ, the average of the two possible values of $Q(\pi,\mu)$ is plotted in figure 7.

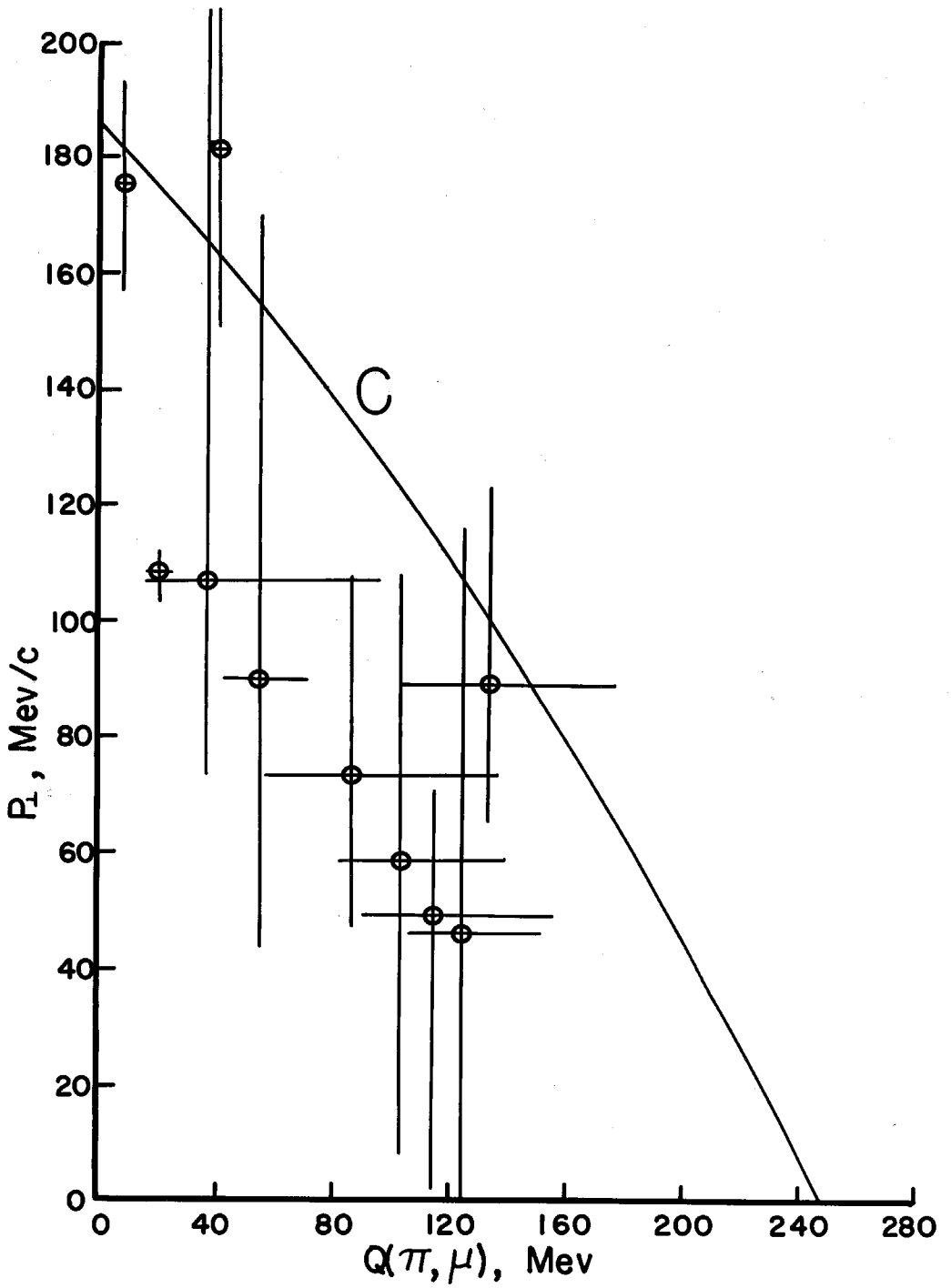
200
180
160
140
120
100
80
60
40
20
0
C
$P_\perp$, Mev/c
0
40
80
120
160
200
240
280
$Q(\pi,\mu)$, Mev

Figure 7

The agreement between the plotted points and the curve is entirely satisfactory, and somewhat better than for scheme B.

$$\text{(D)}\quad \theta^{o}_{anom} \longrightarrow \pi^{\pm} + e^{\mp} + \nu + 354\ \text{Mev}$$

This decay scheme may be the neutral counterpart of the well-established K^{+}_{e3} decay scheme. Event No. 69328, which has an identified electron secondary, may be an example of scheme D. There is also recent evidence[16] from work at Brookhaven for the existence of a V^{o} particle decaying in this way. However, it appears that not all of the events presented here can be explained in this way, since in event 47202 both secondaries are identified as L mesons.

Figure 8 shows a graph similar to the previous ones, constructed by assuming scheme D. For the five events in which either secondary could have been an electron, the value of $Q(\pi, e)$ lying below and closest to the P* curve was chosen. Again, the events are evidently compatible with scheme D on a dynamical basis.

The conclusion which is drawn from the foregoing analysis is that most of the present events cannot be explained by the τ^{o} decay scheme A, but that most, but not all, of the data are consistent with each of the decay schemes B, C, and D.

If the θ^{o}_{anom} particle is assumed to be a K meson, the choice of its mass as 966 m_e is reasonable in view of the

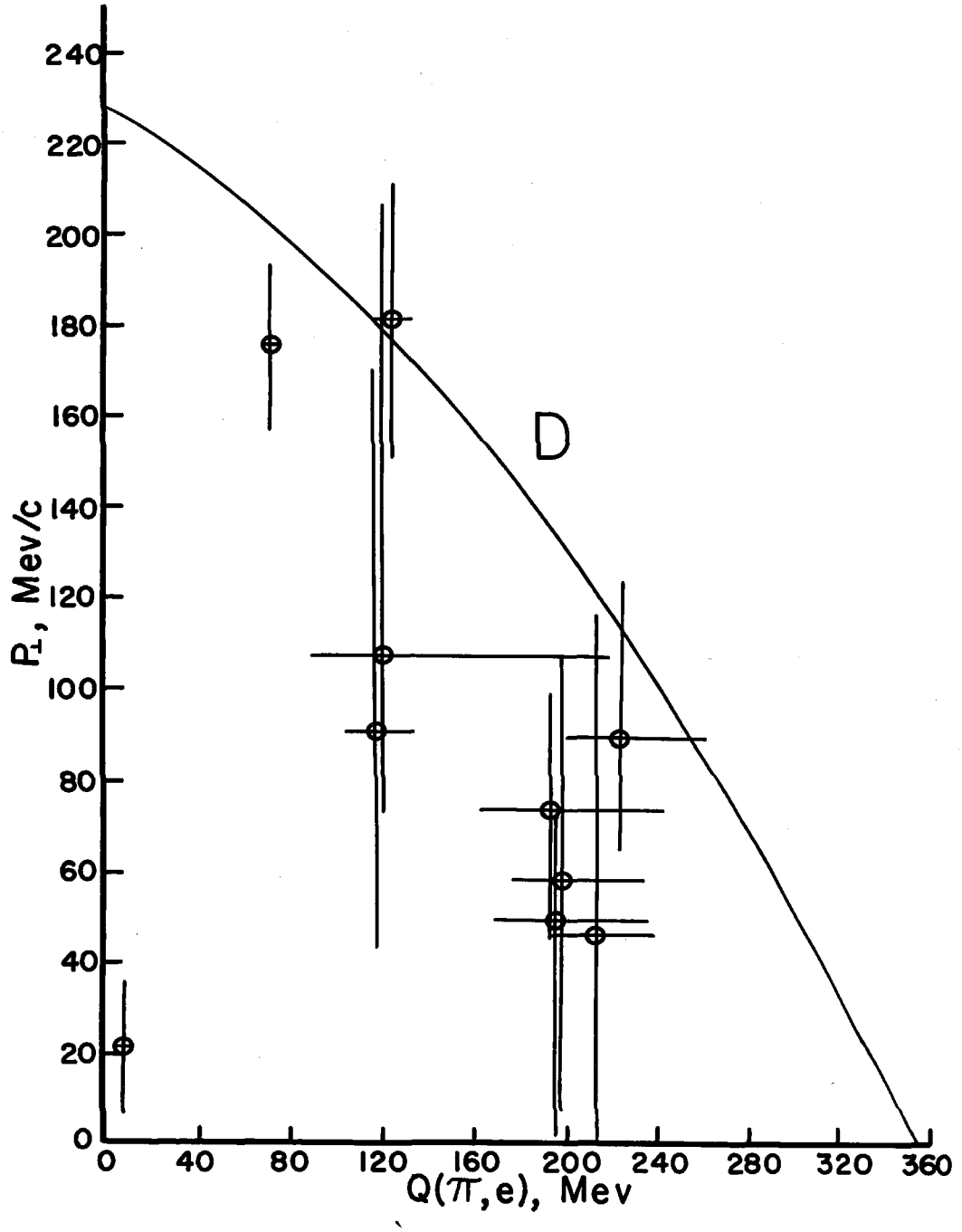
240
220
200
180
160
140
120
100
80
60
40
20
0
$P_\perp$, Mev/c
D
0
40
80
120
160
200
240
280
320
360
Q(π,e), Mev

Figure 8

close agreement between all currently established K-particle masses. However, some additional justification of this mass for the θ^{o}_{anom} particle can be made on the basis of the previously discussed graphs. The curves A through D are rather sensitive to the value assumed for the primary mass. Furthermore, as previously noted, most of the experimental points should cluster close to but below these curves. Thus, if the mass is assumed too small or too large, the data become incompatible with the curves. For example, curve E in figure 6 based upon decay scheme A with an assumed primary mass of 1400 m_e is clearly incompatible with the experimental points.

The interpretation of the θ^{o}_{anom} decays as some form of hyperon decay into a neutron secondary is a possibility that should not be overlooked. However, if the present data are to be explained in this way, one would expect to find a comparable number of corresponding events with a proton secondary, which would be observed as anomalous Λ^{o} decays. Few if any such anomalous Λ^{o} events have ever been detected.

A π^{o} internal conversion into a wide-angle electron pair may have the general appearance of a θ^{o}_{anom} decay if both electrons are too fast to be identified. The π^{o} might, for example, be produced in the neutral decay mode of a Λ^{o}. However, it is found that 2/3 of the present events cannot have originated from π^{o} conversion, based upon the π^{o}-decay dynamics and mass estimates of the secondaries.

V. LIFETIME ANALYSIS

The results of part IV indicate that θ^o_{anom} decays arise from a K^o particle of about the same mass as the $\theta^o_{\pi 2}$. This suggests that θ^o_{anom} decays may be alternate decays of the $\theta^o_{\pi 2}$ particle, in which case the lifetimes as measured for the two particles should be the same. Since the $\theta^o_{\pi 2}$ lifetime has already been measured fairly accurately[17] using the Caltech cloud chambers, a measurement of the θ^o_{anom} lifetime should establish the identity or distinctness of the θ^o_{anom} and $\theta^o_{\pi 2}$ particles.

From a sample of 18 θ^o_{anom} events or less, one cannot hope to measure a precise value for the lifetime, but if the $\theta^o_{\pi 2}$ and θ^o_{anom} lifetimes are quite different there is at least a good chance of distinguishing between these lifetimes.

A. Procedure

In calculating the mean lifetime, the assumption is made that the θ^o_{anom} particle has the same mass as the $\theta^o_{\pi 2}$ particle, viz. 966 m_e. It is also assumed that the decay probability per unit time is a constant, $\frac{1}{\tau}$, independent of the particle's history, so that the resulting distribution of decay times is a decreasing exponential, which for a decay time t and a gate time T is

$$P(t)dt = \frac{1}{\tau} \frac{e^{-t/\tau}}{1 - e^{-T/\tau}} dt \qquad (17)$$

Symbols Used in Further Analysis

x = decay length, distance from point where particle enters illuminated region to decay point.

D = gate length, distance from point where particle enters illuminated region to point on line-of-flight extended where particle could have decayed and still have been identified.

t = decay time = $\frac{x}{\gamma\beta c}$

T = gate time = $\frac{D}{\gamma\beta c}$

P_L, P_L^* = the component of P or P*, respectively, in the direction of the θ^o_{anom} line of flight.

M = apparent mass of θ^o_{anom} particle = $m_1 + m_2 + Q(1,2)$.

E = $\sqrt{P^2 + M^2}$

E^* = $\sqrt{(P^*)^2 + M^2}$

$\Pi(X)$ = detection probability for a given decay event = $e^{-T_L/\tau_x}\left(1 - e^{-T/\tau_x}\right)$, where

τ_x = mean lifetime of particle X.

D_L = distance from origin to point where line of flight enters illuminated region ("distance in lead").

T_L = proper time spent by particle in moving distance D_L

λ = $\sin^{-1}\frac{P^*}{P}$

The decay and gate times for each particle are computed from the particle's momentum, $P_o = \gamma\beta M_o$ and its decay and gate lengths:

$$t = \frac{x}{\gamma\beta c}, \quad T = \frac{D}{\gamma\beta c} \tag{18}$$

The maximum likelihood function for N decay events is then

$$L = \ln \prod_{i=1}^{N} \frac{1}{\tau} \frac{e^{-t_i/\tau}}{1 - e^{-T_i/\tau}} \tag{19}$$

and the maximum likelihood estimate is obtained by putting $\frac{\partial L}{\partial \tau} = 0$:

$$\hat{\tau} = \frac{1}{N} \sum_{i=1}^{N} \left(t_i + \frac{T_i}{e^{T_i/\tau} - 1} \right) \tag{20}$$

The assignment of statistical errors was made by the method of Bartlett,[18] which is a convenient and reliable procedure, even for small samples. In this method, the statistical error, S, is given by the relation

$$\frac{\sum_{i=1}^{N} \left[\frac{t_i}{\tau} - 1 + \frac{T_i}{\tau} \frac{1}{e^{T_i/\tau} - 1} \right]}{\sqrt{\sum_{i=1}^{N} \left[1 - \left(\frac{T_i}{\tau} \right)^2 \frac{e^{T_i/\tau}}{(e^{T_i/\tau} - 1)^2} \right]}} \tag{21}$$

where for any value of τ, $S(\tau)$ gives the number of standard deviations by which τ differs from $\hat{\tau}$. Equation 21 assumes that $S(\tau)$ has a Gaussian distribution, which is nearly true, even for small values of N.

Several important considerations were encountered in the calculation of t_i and T_i: (a) x_i and D_i are not uniquely determined if no origin is present, since the line of flight of the θ^o_{anom} particle is unknown, and (b) $\gamma\beta$ usually cannot be uniquely determined because the decay scheme is not known, and because the momentum of the neutral secondary is unknown. These difficulties will be discussed.

B. Decay and Gate Lengths

If an origin is present, x is measured along the line of flight (L.O.F.) from the edge of the illuminated region of the chamber to the decay point, and D is also measured along the L.O.F. from the same initial point to the last point where the θ^o_{anom} might have decayed with the same orientation and still have been identified. If an origin is not present, the event may still be useful for the lifetime sample. From figure 5 it is seen that the L.O.F. must be within an angle λ of the direction of P, if $P^* < P$, where

$$\lambda = \sin^{-1} \frac{P^*}{P} \qquad (22)$$

Frequently λ is sufficiently small so that the L.O.F. is limited to a narrow cone of directions, making possible measurements of x and D with relatively small error. In such a case, an origin is not necessary, and the event is useful in the lifetime sample.

C. Calculation of $\gamma\beta$

To calculate the lifetime of each θ^{o}_{anom} particle in its own reference frame, it is necessary to know the value of $\gamma\beta = \frac{P_0}{M_0}$, which can be found from the relations*

$$\gamma\beta = \frac{E^* P_L - E P_L^*}{M^2 + P_\perp^2}, \qquad (23)$$

$$\gamma\beta = \frac{E^* \sqrt{P^2 - P_\perp^2} \pm E \sqrt{(P^*)^2 - P_\perp^2}}{M^2 + P_\perp^2}, \quad P > P^* \qquad (23a)$$

$$\gamma\beta = \frac{\pm E^* \sqrt{P^2 - P_\perp^2} + E \sqrt{(P^*)^2 - P_\perp^2}}{M^2 + P_\perp^2}, \quad P < P^* \qquad (23b)$$

All but one of the terms in equation 23 depend upon the choice of the decay scheme. Moreover, even if a particular scheme is assumed, and an origin is present, $P_L^* = \pm \sqrt{(P^*)^2 - P_\perp^2}$ is still indeterminate within a plus or minus sign. If no origin is present, only upper and lower limits can be placed on $P_\perp$, P_L and P_L^*.

These difficulties were handled as follows: Scheme C, $\theta^{o}_{anom} \rightarrow \pi^{\pm} + \mu^{\mp} + \nu$, was used as the basis of calculation for all events,** and then <u>two</u> lifetime calculations were made, one using the maximum value of $\gamma\beta$ ($\gamma\beta_{max}$) for each event, and one using the minimum value ($\gamma\beta_{min}$). This procedure

---

* See Appendix C.

** Except for event 69328, for which scheme D was assumed, since in this decay one secondary is identified as an electron.

was based upon the hope (which was later verified) that the results of the analysis would not be changed if an appreciable number of decays followed schemes B or D instead of scheme C.

The actual lifetime value was expected to lie between the limits established by the two lifetime calculations.* It was also hoped that the lifetime limits obtained using $\gamma\beta_{max}$ and $\gamma\beta_{min}$ would be sufficiently close so that θ^{o}_{anom} lifetime determination would not be seriously limited in precision by the uncertainties in $\gamma\beta$. For a discussion of how $\gamma\beta_{min}$ and $\gamma\beta_{max}$ are determined, see Appendix C.

Occasionally, $\gamma\beta$ can be determined uniquely, if, for example $P_{\perp} = P^*$, in which case the ambiguous term in equation 23a vanishes, or if $P_L < \sqrt{(P^*)^2 - P_{\perp}^2}$, in which case one value of $\gamma\beta$ is negative, and must be rejected.

Table III gives a list of lifetime measurements made upon the events in the lifetime sample.

D. Results of Lifetime Analysis

The θ^{o}_{anom} decay events were selected not by requiring a specific decay scheme, but rather by requiring them to be incompatible with the $\theta^{o}_{\pi 2}$ and Λ^{o} decay schemes. For this

---

* It is possible for a decrease in $\gamma\beta$ for one event to yield a decrease in the calculated lifetime value for the sample of events if the decay time of the event is much shorter than the calculated lifetime value. This is because of the change in the statistical weighting of the event, which also depends upon $\gamma\beta$.

Table III. Lifetime Measurements

Event No.	$\bar{Q}(\pi,\mu)$ (Mev)	P (Mev/c)	$\gamma\beta_{max}$	$\gamma\beta_{min}$	x (cm)	D (cm)	t_{min}	t_{max}	T_{min}	T_{max}
							(In units of 10^{-10} sec)			
				48" Magnet						
19143	40	322	.775		10.6	28.8	4.57		12.4	
31855	9	240	.662	.396	5.6	19.4	2.80	4.68	9.80	16.4
35045	36	452	2.35	.840	2.4	3.3	.338	.994	.465	1.30
36537	~80	~230	.472		2.1	18.3	1.46		13.0	
36894	125	208	.914	.25	5.0	12.4	1.85	6.60	4.60	16.4
37663	126	984	3.44	2.00	9.5	20.6	.83	1.59	1.80	3.44
39522	55	1095	5.18	2.28	10.6	16.2	.68	1.55	1.04	2.37
47202	21	167	1.02		9.5	38.8	3.10		12.7	
56791	133	398	1.16	.820	2.4	19.2	.70	.98	5.55	7.80
57680	88	712	3.18	1.29	5.3	6.3	.55	1.37	.66	1.64
60134	168	523	1.59	.985	5.2	7.3	1.096	1.77	1.53	2.46
69328*	8.3	208	5.06		7.2	16.2	.476		1.07	
				21" Magnet						
10475	115	1827	6.6	3.76	7.1	12.7	.36	.63	.65	1.13
12590	102	807	3.16	1.61	2.0	9.5	.21	.41	1.00	1.97
20923	157	694	1.96	1.46	2.4	8.8	.40	.53	1.49	1.98

* (π^-, e^+) decay was assumed since positive secondary is identified as an e^+.

reason, it is quite possible that the present data represent a mixture of different particles having different lifetimes, (see section VII.B). Accordingly, the calculated mean lifetime value is called τ_{av}, and is some "average" of the lifetimes of the particles present. If a mixture of particles is involved, not all lifetimes can be greater than the upper limit on τ_{av}, and not all lifetimes can be smaller than the lower limit on τ_{av}. Figure 9 shows the resulting likelihood and S functions plotted against reciprocal mean lifetime. The result obtained is:

$$\underset{(\text{max. } \gamma\beta)}{2.9^{+3.0}_{-1.0}} < \tau_{av} < \underset{(\text{min. } \gamma\beta)}{4.4^{+5.3}_{-1.6}} \times 10^{-10} \text{ sec}$$

Standard deviations reflecting the statistical uncertainty are quoted on each lifetime limit. It should be emphasized that the above result does not necessarily preclude the presence of long-lived particles, because (a) this sample probably does contain a mixture of particles of different lifetimes, and (b) even if the sample consists of particles of a unique lifetime, the statistics are insufficient to rule out a relatively long lifetime.

The curves G and I in figure 9 provide a quantitative measure of the agreement of the data with any assumed value for the lifetime. When the Caltech value for the $\theta^0_{\pi 2}$ mean lifetime, 1.3×10^{-10} sec, is chosen, then curve G for $\gamma\beta_{max}$ gives S = 2.5 standard deviations. Consequently, the observed lifetime data are incompatible with the hypothesis

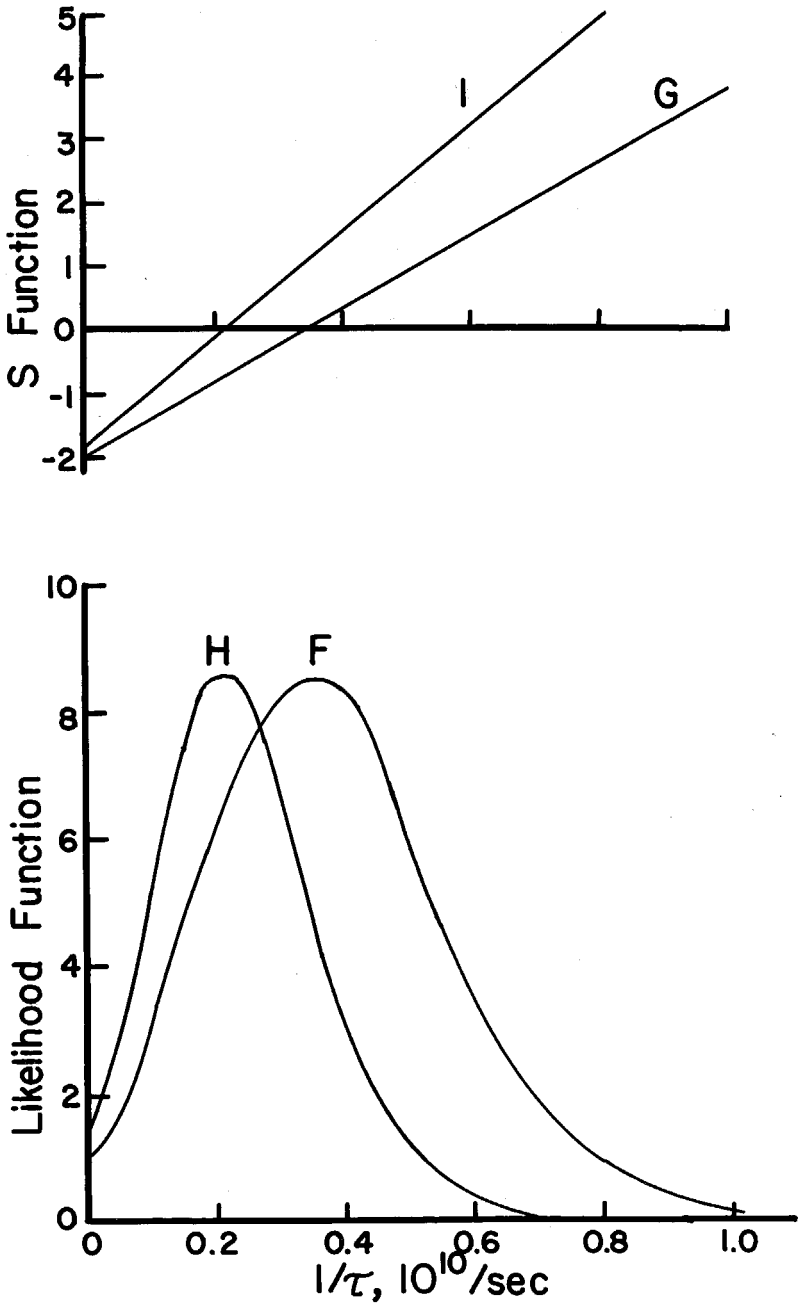
S Function
5
4
3
2
1
0
-1
-2
I
G
Likelihood Function
10
8
6
4
2
0
H
F
0
0.2
0.4
0.6
0.8
1.0
1/τ, 10^10/sec

Figure 9

that this lifetime sample consists entirely of particles having the $\theta^o_{\pi 2}$ lifetime, to a 98 percent significance level. Moreover, this significance level is raised if the $\theta^o_{\pi 2}$ lifetime is actually less than 1.3×10^{-10} sec; this is likely to be the case if the sample of $\theta^o_{\pi 2}$ decays previously used for the lifetime determination was contaminated with a number of high-Q θ^o_{anom} decays, which are experimentally indistinguishable. The above results are taken as evidence for the existence of a θ^o_{anom} particle having a lifetime substantially greater than the $\theta^o_{\pi 2}$ lifetime and for the conclusion that not all θ^o_{anom} decays can be alternate decays of the $\theta^o_{\pi 2}$ particle.

VI. OTHER FEATURES OF θ^o_{anom} vs. $\theta^o_{\pi 2}$ EVENTS*

Certain other properties of the θ^o_{anom} and $\theta^o_{\pi 2}$ particles have been compared, with significant results.* Considerable care always was taken to avoid any influence upon the results by biases resulting from the nature of the 3-body decay.

Table IV summarizes the measurements made upon the origin locations and momenta of θ^o_{anom} and $\theta^o_{\pi 2}$ particles, while table V summarizes the statistics gathered on two other properties: the fraction of θ^o_{anom} and $\theta^o_{\pi 2}$ particles observed traveling upward, and the V particles observed in association with θ^o_{anom} and $\theta^o_{\pi 2}$ particles. These four properties are of particular interest as further evidence against the identity of θ^o_{anom} and $\theta^o_{\pi 2}$ particles, and will be discussed in some detail.

A. Momentum Distributions

As a consequence of the 3-body decay, the average θ^o_{anom} event is more readily distinguished from a Λ^o decay than is a $\theta^o_{\pi 2}$ decay, when the parent particles are of equal momenta. This is a result of lower average momentum of emitted secondaries in the C.M. system, for the θ^o_{anom} decay.

---

* The features discussed in VI.B and VI.C were first pointed out by Dr. G. H. Trilling, while the significance of the associations (section VI.D) was first noticed by Dr. R. B. Leighton.

Table IV. Momentum and Origin Measurements

θ^0_{anom} Particles				$\theta^0_{\pi 2}$ Particles			
Event No.	P_{omax} (Mev/c)	D_L (cm)	$\pi(\theta^0_{\pi 2})$	Event No.	$P_{o\text{max}}$ (Mev/c)	D_L (cm)	$\pi(\theta^0_{\pi 2})$
04480	444	--	--	04417	1410		
19143	382	7.0	.10	04559	1000		
31855	327	8.4	.025	12633	578	8.2	.207
35045	1160	5.1	.248	16393	1775		
*36537	233	7.4	.019	19143	1112	7.0	.440
36894	451	--	--	19731	1195		
37663	1700	5.4	.661	22332	1022		
*39522	2560	24.9	.162	**32100	1100	7.1	.352
45766	870	--	--	32704	390		
47202	504	8.9	.142	33280	850	2.8	.660
56500	651	--	--	33416	507		
56791	571	5.5	.286	35104	1213	5.4	.592
				35286	886		
57680	1570	1.3	.692	40874	2260		
60134	785	--	--	40922	1470	10.0	.435
69328	2500	7.8	.378	41657	2120	4.5	.701
				42317	1189		
				52466	882		
				52687	1385		
				**55432	970	8.0	.400
				56094	3120		
				56614	2010		
				60882	427	3.2	.428
				61265	855	2.6	.618
				61793	1103		
				62803	1935		
				63386	1410		
				63948	655		

* Not used for origin analysis.

** Not used for momentum analysis.

Table V. Statistics on θ^{o}_{anom} vs. $\theta^{o}_{\pi 2}$

A. Numbers of Observed θ^{o}_{anom} and $\theta^{o}_{\pi 2}$ Decays in Which Parent Particle Travels Upward

	$\theta^{o}_{\pi 2}$	θ^{o}_{anom}
Total Number of Observed Decays	238	18
Number in Which Particle Travels Upward	1	4

B. Associations of θ^{o}_{anom} and $\theta^{o}_{\pi 2}$ Particles

	Type of Associated Particle	$\theta^{o}_{\pi 2}$ Associations	θ^{o}_{anom} Associations
Group A	Λ^{o}	10	0
	V^{o}	9	0
	V^{-}	4	0
Group B	K^{+}	1	1
	V^{+}	1	1
	$\theta^{o}_{\pi 2}$	0	1
	K^{-}	0	0
	V^{+}_{-}	1	0

On the other hand, if the $Q(\pi^+, \pi^-)$ value for the decay is much above 100 Mev, the identification bias becomes quite strong against θ^o_{anom} decays, since they cannot be distinguished easily from $\theta^o_{\pi 2}$ decays. These effects have been carefully considered, and in the separation of θ^o_{anom} and $\theta^o_{\pi 2}$ events from Λ^o decays for a comparison of momentum spectra, the criteria discussed below were used. These criteria are felt to be efficient in selecting the most events while not introducing bias in such a way as to influence the result.

1. Momentum vs. Ionization of Positive Secondary

This selection criterion separates Λ^o from K^o particles by the identification of the positive secondary as not a proton. Therefore, a strong bias is present against any particle whose positive secondary has a momentum above about 700 Mev/c. This by itself is no obstacle, since the bias is expected to affect equally the θ^o_{anom} and $\theta^o_{\pi 2}$ momentum distributions. However, an important bias is present due to the difference in the decay processes, as discussed above. Hence, in the higher momentum range, the θ^o_{anom} decays are more easily distinguished from Λ^o decays than are $\theta^o_{\pi 2}$ decays, <u>enhancing</u> this part of the θ^o_{anom} distribution relative to that of the $\theta^o_{\pi 2}$ particle.

---

* These criteria were suggested by Dr. G. H. Trilling.

2. α vs. P

For Λ^0 decays, $\alpha = \frac{P_+^2 - P_-^2}{P_o^2} > 0$ whenever $P_o = P > 300$ Mev/c; this is a consequence of the decay dynamics.[9] Consequently, this criterion is quite useful in separating K^0 from Λ^0 decays at higher momenta, and provides an effective complement to the first criterion. Since α is expected to be negative in about half the cases for both θ^0_{anom} and $\theta^0_{\pi 2}$ decays, there is probably no bias introduced by this criterion.

Having separated out the K^0 particles, it remains to separate them into θ^0_{anom} and $\theta^0_{\pi 2}$ particles with a minimum of intermixing. The following requirements were made:

1. For all θ^0_{anom} events, $Q(\pi^+,\pi^-) \lesssim 125$ Mev and $Q(\pi^+,\pi^-) < 214$ Mev by at least 2 standard deviations.
2. For all $\theta^0_{\pi 2}$ events, $Q(\pi^+,\pi^-) > 125$ Mev by at least 2 standard deviations, and $Q(\pi^+,\pi^-)$ is within one standard deviation of 214 Mev.

These requirements probably eliminated most mixing of the θ^0_{anom} and $\theta^0_{\pi 2}$ events; only a few of the θ^0_{anom} decays from the upper tail of the Q value distribution would be expected to fall into the group with $\theta^0_{\pi 2}$ events.* In addition, the requirement was made that $\theta > 5^\circ$, so that no electron pairs be included in the samples.

---

* See Appendix D for Q value distribution.

Figure 10 shows the results of the momentum analysis. The histogram gives the number of θ^o_{anom} and $\theta^o_{\pi 2}$ particles whose momenta lie within momentum intervals of 400 Mev/c, and is plotted assuming the maximum momentum ($\gamma\beta_{max}$) for each θ^o_{anom} event. The θ^o_{anom} particles clearly have a lower average momentum than the $\theta^o_{\pi 2}$ particles; the difference becomes much more evident if the minimum momentum ($\gamma\beta_{min}$) is used for each θ^o_{anom} event. Furthermore the biases which may be present due to criterion 1, or due to intermixing of θ^o_{anom} and $\theta^o_{\pi 2}$ decays, would tend to make the distributions more nearly the same, and therefore cannot account for the observed difference. A statistical test based upon the number of primary particles of each type having P_o above and below 800 Mev/c shows with 99% significance that the data are inconsistent with the assumption that the momentum distributions of the θ^o_{anom} and $\theta^o_{\pi 2}$ are the same. This result can be understood in terms of a large lifetime difference between the $\theta^o_{\pi 2}$ and θ^o_{anom} particles, and this interpretation will be discussed in part VII.C.

B. Origin Distributions

It is evident from table IV that the origins of low momentum θ^o_{anom} particles are located generally higher in the producing layer of lead above the cloud chamber than are the origins of $\theta^o_{\pi 2}$ particles in the same momentum range. The events used for this comparison were selected according to the criteria discussed in the preceding section. The

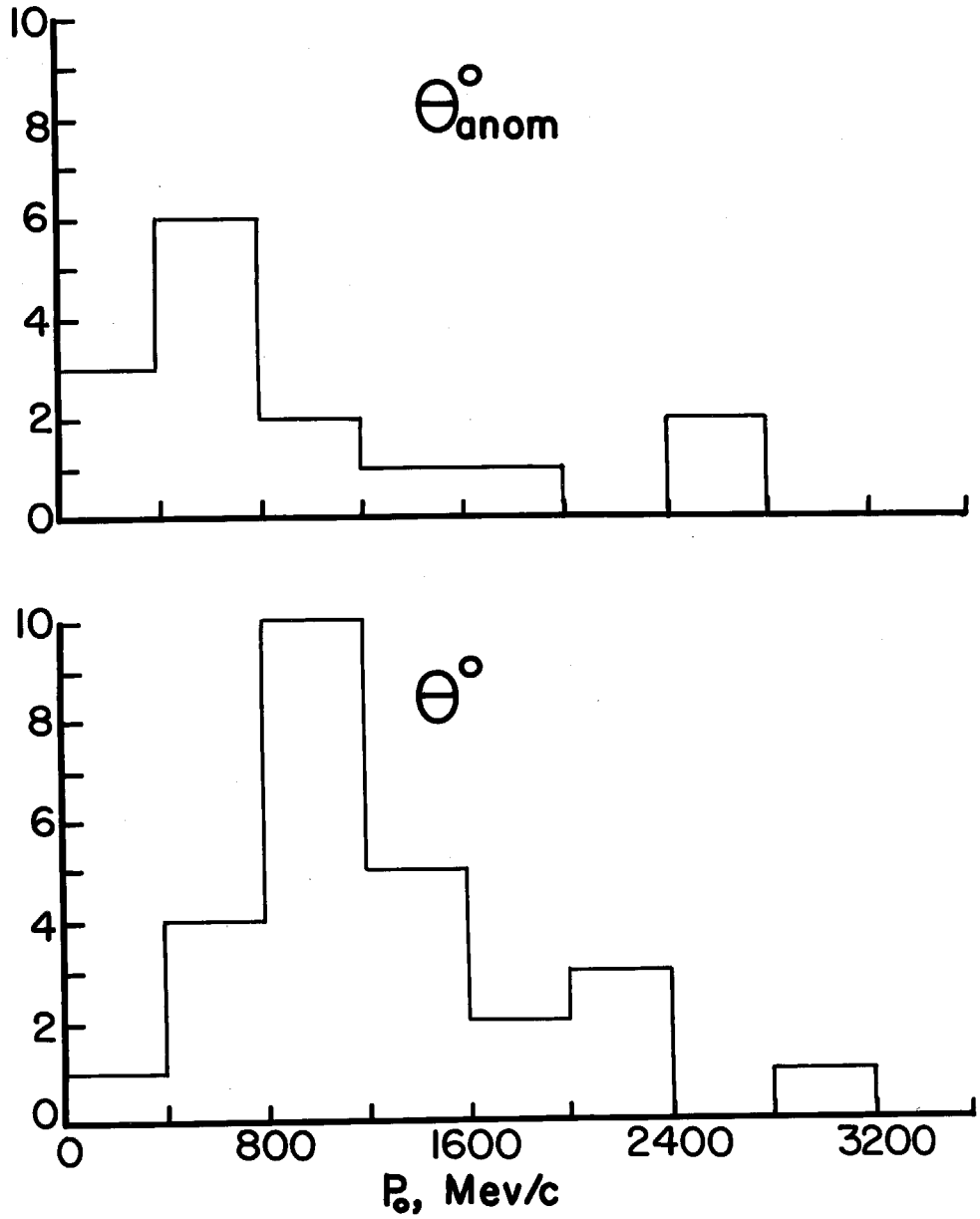

Figure 10

uncertainty in the line of flight of the θ^o_{anom} particles could conceivably lead to incorrect identification of some origins, but an investigation of this effect showed that there is only a small chance of such a mistake (see Section D). In order to minimize this chance, only events were used in which the origin lay within 10 cm. vertical distance of the illuminated region of the chamber.

A more quantitative result was obtained from a statistical test made on the θ^o_{anom} and $\theta^o_{\pi 2}$ samples. To do this, a quantity called $\Pi(\theta^o_{\pi 2})$ was calculated for all sample events. $\Pi(\theta^o_{\pi 2})$ for an event is the a priori probability of decay within the chamber for that particle, based on its origin location and its momentum,* and assuming it to have the $\theta^o_{\pi 2}$ lifetime. For 9 out of the 10 $\theta^o_{\pi 2}$ events, $\Pi(\theta^o_{\pi 2})$ was greater than 30%, while in only 3 out of 8 θ^o_{anom} events was $\Pi(\theta^o_{\pi 2})$ greater than 30%. There is less than one chance in fifty that the values of $\Pi(\theta^o_{\pi 2})$ should be divided as asymmetrically as this if the θ^o_{anom} and $\theta^o_{\pi 2}$ decays actually arise from the same parent particle. This result can also be accounted for by a large lifetime difference.

---

* The maximum momentum, $P_{omax} = \gamma\beta_{max} M_o$, was used for each event. The contrast in the distributions becomes even more striking if $\gamma\beta_{min}$ is used.

C. Upward Moving Particles

One interesting feature of the θ^o_{anom} decays is that the θ^o_{anom} particle is often found to be traveling upward, while $\theta^o_{\pi_2}$ particles do not appear to share this feature. These upward-moving particles are readily detected with the three cloud chambers in the 48" magnet, since interactions frequently occur in the lead plates which separate the chambers. Particles resulting from such an interaction may therefore be seen in the chambers above and below the interaction. To determine the direction of travel of the θ^o_{anom} particle, it is, of course, necessary to make allowance for the neutral secondary in the three-body decay process. Table V shows that at least 4 out of the 18 θ^o_{anom} events are found to be traveling in the upward direction. This result is to be compared with the $\theta^o_{\pi_2}$ events where at most 1 particle is found going upward out of 238 observed $\theta^o_{\pi_2}$ decays, and it is quite conceivable that this one may be a high-Q θ^o_{anom} particle.

Here, then, is a very strong distinction between the θ^o_{anom} and $\theta^o_{\pi_2}$ particles, which may be due to production dynamics, lifetime difference, or possibly other factors. The interpretation of this result is postponed till a later section.

It is interesting to note that in reviewing all the V^o events in an attempt to find more θ^o_{anom} events which might have been missed on the first scannings, 2 of the 3

additional θ^o_{anom} particles discovered were spotted because they were moving upward.

D. Associated Decay Events

If the θ^o_{anom} and $\theta^o_{\pi 2}$ decays arise from the same particle, then they should be associated with the same types of V-particle decays. Among the 18 events, there are 3 where another V particle decays and appears to be associated with the θ^o_{anom} particle. These associations are summarized in table V. Even though the statistics are limited, the differences in associations are rather striking.

Due to the uncertainty in the line of flight, the assignment of the correct origin for a θ^o_{anom} particle is more uncertain than for a $\theta^o_{\pi 2}$ particle. Consequently, there is reason for legitimate concern regarding the authenticity of the 3 associations. It was found that all 3 events are dynamically quite consistent with what appear to be their correct origins. However, in order to seek greater confidence in the results, a detailed investigation was made to determine the probability of incorrect origin identification. An examination was made of all events where 2 or more V particle decays of any kind were seen together in the same chamber. Since these events consist almost entirely of two-body decays, the lines of flight are well defined, and it was relatively easy to determine in what fraction of the cases the par-

ticles were not truly associated, but happened to come from different origins which were closely spaced. The results of this examination are:

Number of Associations	68
Number of Probable Associations	11
Number of Probable Non-associations	6
Number of Non-associations	13
Average Distance Between Origins of Non-associated Particles	13 cm

These figures indicate that probably not more than about 1/5 of the multiple V events have non-associated decays. By defining for each of the 3 θ^{o}_{anom} associated events a region including all visible interactions from which the θ^{o}_{anom} particle could have originated, and by comparing these regions to the 13 cm. average distance between origins of non-associated particles, an estimate was made of the chance of non-association. The result was that the maximum number of non-associations expected from the 3 events was only 0.3.

An estimate was made also in another way, by examining all multiple V events in which a $\theta^{o}_{\pi 2}$ decay was identified, or where a V^{o} decay occurred which could have been a $\theta^{o}_{\pi 2}$. A total of 73 such events was found. Among these 73 events, the maximum number was found of non-associated events which could have been mistaken as associations if a θ^{o}_{anom} decay had occurred instead of a $\theta^{o}_{\pi 2}$ decay. Nine such events were found. Therefore, not more than about 1/8 of the θ^{o}_{anom} as-

sociations should be false, or about $3/8 \simeq 0.4$ of the present θ^{o}_{anom} associations. This agrees well with the previous estimate.

An effect which may be of importance but has not been discussed is that of correlation between origin locations. Since V particles are frequently produced in penetrating showers, an appreciable chance might exist that more than one V particle origin might occur within the core of a shower, or even within the same nucleus, so that the closely localized origins would be indistinguishable. It is difficult to estimate this effect, except to say that out of 18 associations involving Λ^{o} particles,[19] there is not one case of (Λ^{o}, Λ^{o}) association, indicating that origins may not frequently occur close together.

In order to express in more quantitative terms the apparent difference between the associations, a statistical test was made in the following way. Two groups of associated events were formed: group A consisted of the most prevalent associations of the $\theta^{o}_{\pi 2}$, viz. the Λ^{o}, V^{o}, and the V^{-}, while group B consisted of the remaining associations in table III. While 23 out of the 26 $\theta^{o}_{\pi 2}$ associated decay events occur in group A, none of the 3 θ^{o}_{anom} associations falls in group A. If we assume that the types of associations should be the same for the $\theta^{o}_{\pi 2}$ and θ^{o}_{anom} events, then the probability that a disparity as great as this should exist between the observed associations is only 0.005. A discussion of the possible effects of production dynamics

upon the observed associations, and of a lifetime bias on all of the preceding results of part VI will be given in part VII.D.

In summary of the foregoing analysis, it is concluded that θ^{o}_{anom} and $\theta^{o}_{\pi 2}$ decays are not alternate decay modes of the same particle.

E. Mixture of τ^{o} Decays and Alternate Decays of $\theta^{o}_{\pi 2}$

The previous discussion does not rule out the possibility that the θ^{o}_{anom} decays may be explained partly by the τ^{o} decay scheme, and partly by alternate decay modes of the $\theta^{o}_{\pi 2}$ particle. However, some of the previous arguments may also be used to show that this explanation is not adequate, since a number of θ^{o}_{anom} decays do not fit either interpretation:

1) The lifetime has been calculated from 10 θ^{o}_{anom} events which are inconsistent with the τ^{o} decay scheme by at least one standard deviation in Q and $P_{\perp}$ from the values appropriate to the τ^{o} decay scheme. The resulting likelihood function and S function are shown in figure 11. Even though the statistics are limited, it was found that with 94 percent significance, the lifetime data are inconsistent with the $\theta^{o}_{\pi 2}$ lifetime of 1.3×10^{-10} seconds.

2) As was pointed out in section IV.3.3, the four events in which the θ^{o}_{anom} is traveling upward are quite unlikely to be alternate decays of a $\theta^{o}_{\pi 2}$. However, two of these events are also dynamically inconsistent with the τ^{o}

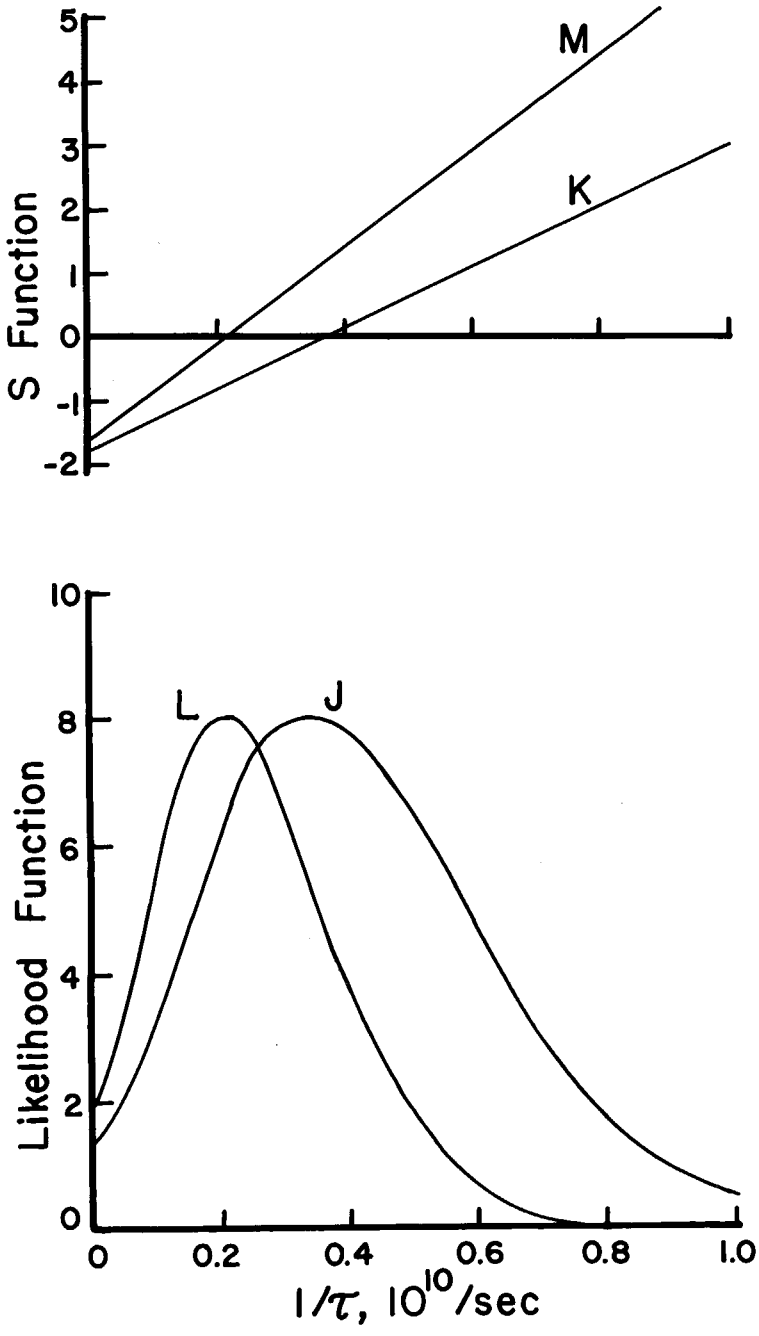
S Function
5
4
3
2
1
0
-1
-2
M
K
Likelihood Function
10
8
6
4
2
0
L
J
0
0.2
0.4
0.6
0.8
1.0
1/τ, 10^10/sec

Figure 11

decay scheme by more than two standard deviations, and a third has a $Q(\pi^+,\pi^-)$ value greater than 80 Mev by more than one standard deviation.

3) In the previous section, it was shown that the observed associations are very unlikely if the θ^o_{anom} events with associations were alternate decays of the $\theta^o_{\pi 2}$. Moreover, the decay dynamics are such that all three θ^o_{anom} events with associated decays are inconsistent with the τ^o decay scheme by at least two standard deviations.

From these arguments, one concludes that all θ^o_{anom} events cannot be explained as simply a combination of the τ^o decay scheme and the alternate decay modes of the normal $\theta^o_{\pi 2}$.

VII. INTERPRETATION OF θ^o_{anom} EVENTS

Inasmuch as the experimental evidence strongly opposes explanation of θ^o_{anom} decays on the basis of any known particles, a new V^o particle must be acknowledged. However, the nature of this new particle is still rather obscure, and considerably more information should be forthcoming on its properties, such as cross-section, associations, decay modes, and precise lifetime and mass, before it is considered a well-understood particle. In the following discussion, various interpretations of the nature of the θ^o_{anom} particle will be explored.

One possibility is that the θ^o_{anom} is the τ^o particle* decaying by one of the modes B, C or D (see section IV.B), since these decays are more probable than mode A on the basis of the phase space available to the decays. However, another explanation very unique in nature appears to show considerable evidence of being correct and will be discussed in some detail.

A. The Gell-Mann, Pais Theory of θ^o_1 and θ^o_2 Particles[6]

A set of experiments first performed at the Brookhaven National Laboratories[16] indicate that the θ^o meson and its antiparticle, $\overline{\theta^o}$, are distinct in strong interactions, such

---

* Recent experiments on parity indicate that the τ and θ particles may be identical, in which case this paragraph loses its significance.

as the production process. The reaction

$$\pi^- + P \longrightarrow \Lambda^\circ + \theta^\circ \qquad (24)$$

was observed to occur with large cross-section, while the reaction

$$N + N \longrightarrow \Lambda^\circ + \Lambda^\circ \qquad (25)$$

was unobserved, and presumably forbidden. However, the Yukawa process $\pi^- + P \rightleftharpoons N$ together with reaction 1 permits the reaction

$$N + N \longrightarrow \Lambda^\circ + \Lambda^\circ + \theta^\circ + \theta^\circ \qquad (26)$$

If $\bar{\theta}^\circ \equiv \theta^\circ$, then the $\bar{\theta}^\circ$ and θ° mesons may annihilate in virtual states, and the result is reaction 25. The absence of reaction 25 is therefore indirect evidence for the conclusion that $\bar{\theta}^\circ \equiv \theta^\circ$.

However, this conclusion seems not to be rigorously binding, for the decay process

$$\theta^\circ \longrightarrow \pi^+ + \pi^- \qquad (27)$$

is changed by application of the charge conjugation operation into

$$\bar{\theta}^\circ \longrightarrow \pi^- + \pi^+ \qquad (28)$$

where the mesons are in same state, and so the process

$$\theta^{\circ} \rightleftharpoons \pi^{+} + \pi^{-} \rightleftharpoons \overline{\theta}^{\circ} \qquad (29)$$

exists, at least as a virtual process, and the distinctness of θ° and $\overline{\theta}^{\circ}$ is apparently not preserved in the weak processes, such as decay.

This seems to be a novel situation, for previously all neutral elementary particles appeared to be always either distinct from or identical with their antiparticles. The neutron, for example, is apparently always distinct from the antineutron, due to the rigorously exact (so far as is known) conservation of baryon number. In the present instance, however, the θ° and $\overline{\theta}^{\circ}$ states are mixed by the weak interactions.

By assuming charge conjugation to be invariant in both weak and strong interactions,* it becomes clear that the $\theta^{\circ}_{\pi 2}$ particle has a definite charge conjugation quantum number, C, while the θ° and $\overline{\theta}^{\circ}$ do not have. Let $\mathcal{C}$ = charge conjugation operator, and ψ = wave function for the θ° meson; then $\psi^{\dagger} = \mathcal{C}\psi$ is the hermitian of ψ, and represents the antiparticle, $\overline{\theta}^{\circ}$. By combining ψ and $\psi^{\dagger}$ suitably

---

* Recent experiments indicate that charge conjugation and parity may not be invariant in the presence of weak interactions. However, this will not alter the conclusions if parity and charge conjugation together form an invariant. Furthermore, it has been shown by Lee, Yang, and Oehme, that even if CP is not an invariant, the observed long lifetime of θ°_{anom} guarantees that the situation is not much different from what is described here.

(mixing θ^o and $\overline{\theta^o}$), two states, θ_1^o and θ_2^o, are created having definite values of C:

$$\theta_1^o = \frac{1}{\sqrt{2}}(\psi + \psi^t), \quad C\theta_1^o = +\theta_1^o, \quad C = +1 \tag{30}$$

$$\theta_2^o = \frac{1}{i\sqrt{2}}(\psi - \psi^t), \quad C\theta_2^o = -\theta_2^o, \quad C = -1 \tag{31}$$

One of these states, and only one, decays by the $\pi^+ + \pi^-$ mode, which has $C = (-1)^{\ell}$, where $\ell\hbar$ is the spin angular momentum of the $\theta_{\pi 2}^o$ particle. Assume $\ell = 0$, so that for the $\theta_{\pi 2}^o$ decay, C = +1, and

$$\theta_1^o \longrightarrow \pi^+ + \pi^- \tag{32}$$

Since the θ_2^o must have the same spin as the θ_1^o (here taken as zero), the θ_2^o <u>cannot</u> decay by the mode 32, and therefore decays by other modes, such as three-body decays, and probably has a much longer lifetime than the θ_1^o lifetime.

On the other hand the θ^o and $\overline{\theta^o}$ mesons are composed of mixtures of the θ_1^o and θ_2^o states,

$$\psi = \frac{1}{\sqrt{2}}(\theta_1^o + i\theta_2^o), \qquad \psi^t = \frac{1}{\sqrt{2}}(\theta_1^o - i\theta_2^o) \tag{33}$$

and thus have no definite value of C. Since the value of C determines the observed types of decays, the unique lifetime must be ascribed to the states with definite values for C, i.e. the θ_1^o and θ_2^o. The term "particle" is properly reserved for the entity having unique lifetime, and so the θ_1^o and θ_2^o are particles, while the θ^o and $\overline{\theta^o}$ are particle

mixtures by relations 33. However, the θ_1^o and θ_2^o should have identical spin, momentum distribution, angular distribution, associations, and all features related to the production process, for they are always produced together according to relations 33, and they are expected to have nearly identical masses. According to this scheme, the $\theta_{\pi 2}$ decay can originate from either the θ^o or $\overline{\theta^o}$ mesons.

It is apparent that most of the features of the θ^o_{anom} events can be readily explained by interpreting the θ^o_{anom} as the θ_2^o, and the $\theta^o_{\pi 2}$ as the θ_1^o: the θ^o_{anom} decays clearly have three or more secondary particles, and the lifetime is longer, perhaps much longer, than that of the $\theta^o_{\pi 2}$. Furthermore, a pronounced lifetime difference between the $\theta^o_{\pi 2}$ and θ^o_{anom} might well be sufficient to account for the observed differences in the momentum distributions and origin locations, the comparatively large fraction of θ^o_{anom} primaries traveling upward, and perhaps even for the apparent differences in associations of the $\theta^o_{\pi 2}$ and θ^o_{anom}.

B. Lifetime Estimate of θ_2^o

If the θ^o_{anom} decays are assumed to arise from the θ_2^o particle, and $\theta^o_{\pi 2}$ decays from the θ_1^o particle, then an estimate can be made of the θ_2^o lifetime, based upon the relative numbers of observed θ^o_{anom} and $\theta^o_{\pi 2}$ decays. For this purpose, the following symbols are defined:

N_o = total number of θ^o and $\overline{\theta^o}$ mesons produced, expected to be half θ_1^o and half θ_2^o particles.

N_1 = number of $\theta^o_{\pi 2}$ decays observed.

N_2 = number of θ^o_{anom} decays observed which arise from θ^o_2 particles.

Brackets around the last two symbols indicate the expected number, e.g. $\langle N_2 \rangle$.

$\rho_{1,2}$ = fraction of θ^o_1 or θ^o_2 decays which occur by the $\theta^o_{\pi 2}$ or θ^o_{anom} modes, respectively.

$\pi_{1,2}$ = detection probability for $\theta^o_{\pi 2}$ and θ^o_{anom} decays, respectively.

$T_{1,2}$ = gate time for $\theta^o_{\pi 2}$ and θ^o_{anom} particles, respectively.

A bar over the last two symbols indicates the statistical average over all observed particles, e.g. $\overline{\pi_1}$.

$\tau_{1,2}$ = mean lifetime of θ^o_1 and θ^o_2 particles, respectively.

The following relations are expected to be true:

$$\langle N_1 \rangle = \tfrac{1}{2} N_o \rho_1 \overline{\pi_1}$$

$$\langle N_2 \rangle = \tfrac{1}{2} N_o \rho_2 \overline{\pi_2}$$

If T_2 is at least somewhat less than τ_2 for all θ^o_{anom} events, then the approximation can be made:

$$\pi_2 \simeq (1 - e^{-T_2/\tau_2}) \simeq \frac{T_2}{\tau_2}$$

The averages are made by weighting each event inversely as its detection probability:

$$\overline{\pi_1} = \frac{\sum_{k=1}^{N_1} \left(\frac{1}{\pi_{1k}}\right) \pi_{1k}}{\sum_{k=1}^{N_1} \left(\frac{1}{\pi_{1k}}\right)} = \frac{N_1}{\sum_{k=1}^{N_1} \left(\frac{1}{\pi_{1k}}\right)}$$

Similarly:

$$\overline{\pi_2} = \frac{N_2}{\sum_{k=1}^{N_2} \left(\frac{1}{\pi_{2k}}\right)} \simeq \frac{T_2}{\tau_2}$$

since

$$\overline{T_2} = \frac{\sum_{k=1}^{N_2} \left(\frac{1}{\pi_{2k}}\right) T_{2k}}{\sum_{k=1}^{N_2} \left(\frac{1}{\pi_{2k}}\right)} \simeq \frac{\sum_{k=1}^{N_2} \left(\frac{\tau_2}{T_{2k}}\right) T_{2k}}{\sum_{k=1}^{N_2} \left(\frac{1}{\pi_{2k}}\right)} = \frac{\tau_2 N_2}{\sum_{k=1}^{N_2} \left(\frac{1}{\pi_{2k}}\right)} \simeq \frac{N_2}{\sum_{k=1}^{N_2} \left(\frac{1}{T_{2k}}\right)}$$

Combining these relations, and using N_1 and N_2 to estimate $\langle N_1 \rangle$ and $\langle N_2 \rangle$, respectively,

$$\frac{N_2}{N_1} \sim \frac{\langle N_2 \rangle}{\langle N_1 \rangle} = \frac{\rho_2}{\rho_1} \frac{\pi_2}{\pi_1} \simeq \frac{\rho_2}{\rho_1} \frac{T_2}{\overline{\pi_1}} \frac{1}{\tau_2}$$

or

$$\tau_2 \simeq \frac{\rho_2}{\rho_1} \frac{\overline{T_2}}{\overline{\pi_1}} \frac{N_1}{N_2} \qquad (34)$$

An estimate of τ_2 can be obtained, provided the quantities on the right of equation 34 can be determined. However, N_2 is really an upper limit on the number of observed θ_2^o decays, since θ_{anom}^o decays may, and probably do, arise

from sources other than the θ_2^o particle (e.g. $\theta_1^o \rightarrow \pi^{\pm} + \mu^{\mp} + \nu$ may have the same decay rate as the θ_2^o particle decaying by this mode). Also, ρ_1 and ρ_2 are not accurately known at present, but ρ_2 is probably quite close to unity, and ρ_1 cannot be greater than unity. Thus, a more meaningful result is obtained by finding a lower limit on τ_2 by letting $\frac{\rho_2}{\rho_1} = 1$ and using for N_2 the number of all observed θ^o_{anom} decays, selected according to suitable criteria.

Since certain particles and decay modes are much more readily identified than others, it was necessary to consider the effects of various biases, arising from such characteristics as lifetime and the 3-body nature of the θ^o_{anom} decay. Because of the relatively short and long lifetimes of the $\theta^o_{\pi 2}$ and θ^o_{anom} particles, respectively, most $\theta^o_{\pi 2}$ decays occur near the top of the chamber, whereas θ^o_{anom} decays are distributed more or less uniformly throughout the chamber. However, a particle which decays near the bottom of the chamber can seldom be classified because of the short secondary track lengths. Therefore, only particles which decayed in the upper half of the chamber were used. Since θ^o_{anom} particles tend to be slower than $\theta^o_{\pi 2}$ particles, the criteria by which events are selected must be uncorrelated with the particle's momentum. Also, the criteria must not depend to a large degree on whether the decay occurs by a 2-body or 3-body mode. One criterion used was that $\alpha \leq 0$ for $P > 400$ Mev/c. The number of events found in this way must be doubled to obtain the total num-

ber of decays, since as many are expected to have $\alpha > 0$ as $\alpha < 0$. For events with $P \leq 400$ Mev/c, all events are sufficiently easy to identify that little bias exists, and any of the methods of identification may be used. The additional requirement was made that $\theta > 5^{\circ}$, to avoid any electron pairs from γ conversion, and an origin was required within 10 cm. vertical distance of the illuminated region. The latter requirement insured that the particles originated in the same producing layer of lead. The separation into θ^{o}_{anom} and $\theta^{o}_{\pi 2}$ decays was made by dividing all events into two groups, having $Q(\pi^{+},\pi^{-})$ values above and below 65 Mev. When the $Q(\pi^{+},\pi^{-})$ of an event was not accurately measurable by momentum measurements, the following relation between P and θ was used, which is a good approximation for a reasonably large group of events:*

$$P \tan \theta \leq 400, \quad \text{for} \quad Q(\pi^{+},\pi^{-}) \leq 65 \text{ Mev} \qquad (35)$$

A correction can now be made for the two-thirds of the θ^{o}_{anom} decays expected to occur with $Q(\pi^{+},\pi^{-}) > 65$ Mev, based upon the Q value distribution,* to obtain an estimate of the true numbers of observed θ^{o}_{anom} and $\theta^{o}_{\pi 2}$ decays. A summary of the calculations made for each event used is found in table V. Although only two θ^{o}_{anom} events qualified for the analysis, three more were found which did not

---

* See Appendix D.

qualify because of origin or Q value requirements. These additional events were used to obtain a more significant value of $\overline{T}_2$, since no important correlation is expected to exist between T_2 and these requirements. The results of the calculations are:

$$N_1 = 52,\ N_2 = 6;\ \overline{\pi}_1 = 0.42,\ T_2 = 3.3\times10^{-10} \text{ sec.}$$

$$\tau_2 > \frac{N_1}{N_2}\frac{\overline{T}_2}{\overline{\pi}_1} = \frac{52}{6}\ \frac{3.3\times10^{-10}}{0.42} \text{ sec} = 0.7\ {}^{-0.33\times10^{-8}} \text{ sec}$$

where a probable error has been quoted for the lower limit; no upper limit is given since this would require knowledge of how many decays arise from particles other than the θ_2^o. However, if all θ_{anom}^o decays arise from the θ_2^o particle, an upper limit on τ_2 is $\sim10^{-7}$ sec.

Because of the large statistical uncertainty, the lower limit on τ_2 is not completely inconsistent with τ_{av}, but is sufficiently greater than τ_{av} to indicate that some short-lived events may be present in the θ_{anom}^o lifetime sample. As proposed earlier, such events may be 3-body decays of the θ_1^o particle.

C. Influence of Lifetime upon Experimental Results

From the preceding discussion, it appears likely that if the θ_2^o exists as postulated, it probably has a much longer lifetime than the θ_1^o particle, and the preceding experimental results have been re-examined in the light of this evidence to see if they can be explained solely by the existence of the θ_2^o particle.

1. Momentum Distributions

The lower average momentum observed for the θ^o_{anom} particle than for the $\theta^o_{\pi 2}$ particle can be easily understood qualitatively as a consequence of a large lifetime difference between the particles. Since the mean decay length of a 800 Mev/c $\theta^o_{\pi 2}$ particle is about 6 cm, while the average origin distance from the chamber is somewhat over 6 cm, it is clear that the flux of $\theta^o_{\pi 2}$ particles will be rapidly attenuated by decay before reaching the chamber as P_o drops below 800 Mev/c. On the other hand, the detection probability for θ_2^o particles, $\pi(\theta_2^o)$, will be inversely proportional to momentum, nearly, since

$$\pi(\theta_2^o) \simeq \frac{T}{\tau_2} = \frac{M_o}{P_o}\,\frac{D}{c\tau_2}$$

Because τ_2 appears to be large compared with T in most cases, evidently only the slowest θ_2^o decays have an appreciable chance of being observed. In such a way, the lifetime difference causes an effective separation of the θ_1^o and θ_2^o decays into high and low momentum groups, respectively.

2. Origin Distributions

The same lifetime bias discussed above also discriminates against slow θ_1^o particles whose origins are located high in the production layer, since few such particles survive to reach the chamber. There is no such discrimination against the long-lived θ_2^o particle.

3. Upward-Moving Particles

The effect of lifetime bias upon the observed direction of travel can be very large, since the speed of the particle produced depends to a large degree upon its direction of travel relative to the path of the producing particle. Since most V particles are produced by downward-moving particles, the θ^o mesons emitted upward have relatively low momentum, while those emitted downward have high momenta. In the light of the discussion of the preceding sections, one would expect a lifetime bias to favor long-lived particles, such as the θ_2^o, among the observed slow, upward moving particles, while the shorter-lived θ_1^o particles should have a greater detection probability when emitted in the downward direction.

Although table V shows the disparity between the fraction of θ_{anom}^o and $\theta_{\pi 2}^o$ particles observed traveling upward to be very great, a more significant comparison should be between particles in the same momentum range, in view of the correlation between momentum and direction of travel.

Among the particles having momenta less than 600 Mev/c, for example, 4 out of 7 θ^o_{anom} and at most 1 out of 4 $\theta^o_{\pi 2}$ particles travel upward. The discrepancy is not so large now, and can be understood by a lifetime bias.

Another approach is to compute from the events in which the θ^o_{anom} particle is moving upwards, the expected number of $\theta^o_{\pi 2}$ decays. A correction was made for the difference in detection probabilities for the two decays by computing $\frac{\pi(\theta_1^o)}{\pi(\theta_2^o)}$ for each of the 3 events having origins. The result is that about 2 $\theta^o_{\pi 2}$ decays should have been observed from upward-moving particles, not allowing for the possible decays $\theta^o_1 \rightarrow \pi^o + \pi^o$, which may occur as often as the $\theta^o_{\pi 2}$ decay.[20] If such decays do occur, about one $\theta^o_{\pi 2}$ decay should be seen, and one <u>is</u> observed.

4. Associations of θ^o_{anom} and $\theta^o_{\pi 2}$

Since the associations of the θ^o_1 and θ^o_2 particles should be identical, the very large difference between the observed types of associations, summarized in table V, is difficult to explain purely on the assumption that $\theta^o_1 \equiv \theta^o_{\pi 2}$ and $\theta^o_2 \equiv \theta^o_{anom}$. Neither can the results be easily explained as being accidental associations, as was previously pointed out. Consequently, an attempt was made to ascertain the possible influence of various biases. If such biases do not provide an adequate explanation, then some other physical basis for the effect must be sought.

The $\theta^o_{\pi 2}$ associations are in approximate agreement with

the expected results. Associations of the $\theta^o_{\pi 2}$ with the shorter-lived hyperons, such as Λ^o, Σ^- are expected to be seen more frequently than K^+ associations, because of the lifetime bias. Furthermore, K^- particles are discriminated against not only because of lifetime, but because of higher threshold energy required and probably because of smaller production cross-section, since a K^- can be produced only with another K particle. The presence of one ($\theta^o_{\pi 2}$, K^+) and absence of any ($\theta^o_{\pi 2}$, $\theta^o_{\pi 2}$) can be partly understood on the basis of the large probability of a θ^o meson decay through the "invisible" modes $\theta^o_1 \rightarrow \pi^o + \pi^o$ and $\theta^o_2 \rightarrow \theta^o_{anom}$ decay (indeed, one of the latter decays has been seen). Based upon the strangeness classification in figure 12, and the preceding discussion a reasonable guess can be made as to the nature of unidentified $\theta^o_{\pi 2}$ associations: The V^o are nearly all Λ^o decays, while the V^+_- are nearly all $\Sigma^\pm$ decays.

The absence of θ^o_{anom} associations in group A of table V is unaccountable except by a very strong bias, since the θ^o meson produced with the hyperons of group A should decay as often via the θ^o_1 route as by the θ^o_2 or θ^o_{anom} mode; furthermore, a significant branching ratio for the $\theta^o_1 \longrightarrow \pi^o + \pi^o$ decay[20] <u>increases</u> the chance of θ^o_{anom} associations in group A by perhaps a factor of two. On the other hand, for origins which are more than a few centimeters from the illuminated region of the chamber, a lifetime bias affects the associations to cause long-lived

UNSTABLE PARTICLE DECAYS

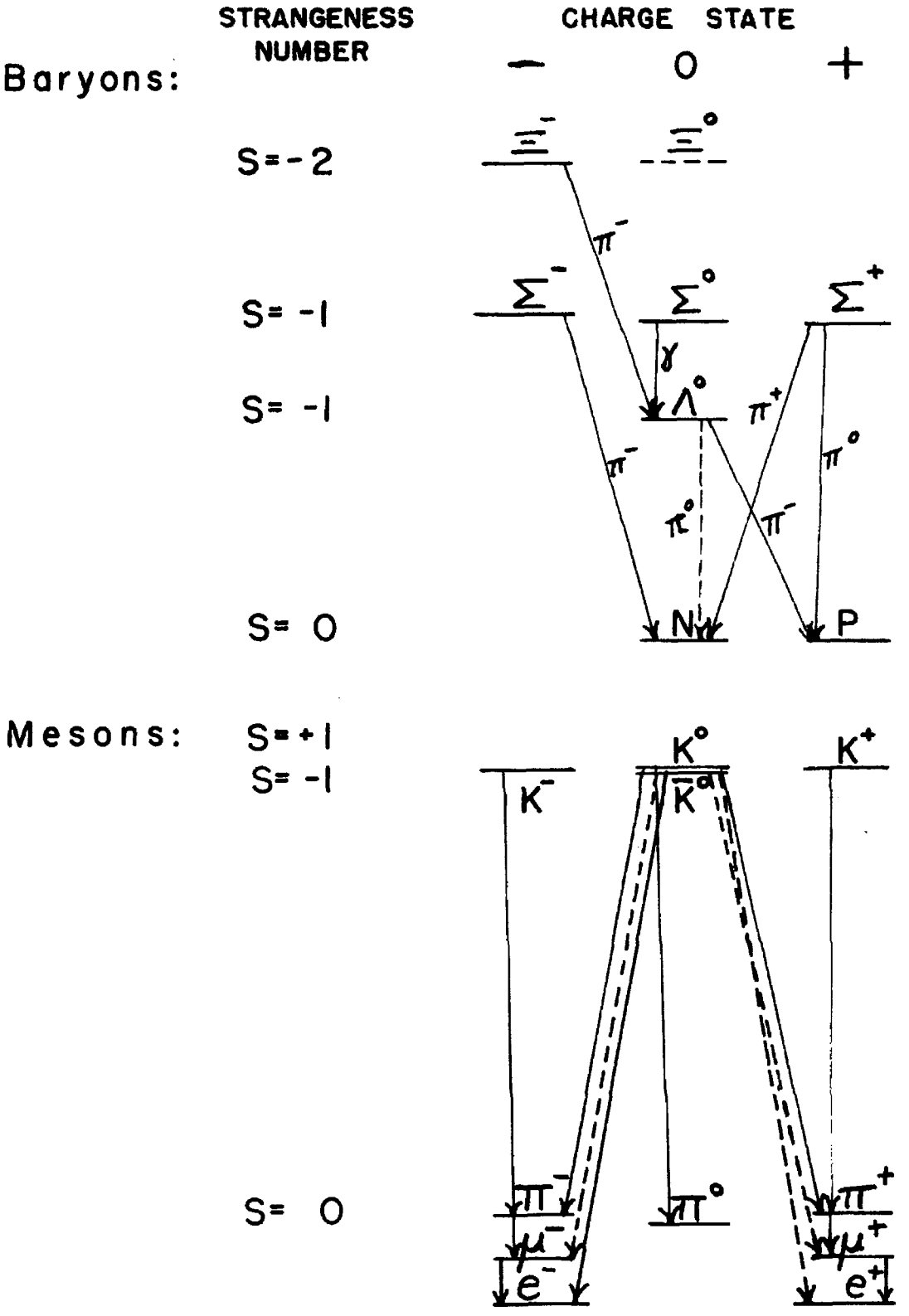

Figure 12

Predicted but unconfirmed particles are indicated by dashed lines

particles to be observed primarily with long-lived particles, and short-lived with short-lived. This is because the V particles produced together are correlated in momentum; if the production is caused by a very energetic primary, both V particles have high momentum on the average (assuming isotropic production in the C.M. system) while production just above threshold results in low-momentum particles. As has been seen previously, the lifetime bias is quite effective in separating particles of different lifetime, according to their momenta. An additional effect probably reinforces this bias: this is preferred backward emission of Λ° particles in the C.M. system during production, which has been reported by at least three different sources.[21,22,23] This would cause an even greater discrimination between the observed Λ° associations, since the θ° being thrown forward has a higher momentum, and the result is that $\pi(\theta_1^\circ)$ is increased and $\pi(\theta_2^\circ)$ decreased.

In order to estimate the effects of these biases, all the $\theta^\circ_{\pi 2}$ associations of group A were studied in detail. Assuming that the branching ratio is $\frac{1}{2}$ for the process $\theta_1^\circ \rightarrow \pi^+ + \pi^-$ and unity for $\theta_2^\circ \rightarrow$ charged secondaries, and assuming θ_1° and θ_2° lifetimes of 1.3×10^{-10} sec. and 1.0×10^{-8} sec., respectively, the ratio $2\,\frac{\pi(\theta_2^\circ)}{\pi(\theta_1^\circ)}$ computed for each $\theta^\circ_{\pi 2}$ event is an estimate of the chance that a θ°_{anom} decay would have been observed instead. The sum

of these ratios for the 23 $\theta^o_{\pi 2}$ associations of group A was 1.14. However, only the high-momentum $\theta^o_{\pi 2}$ particles are observed, because of lifetime bias, and so an estimate was also made in the low-momentum range by examining the (K^+, Λ^o) and (K^+, V^o) associations. Only 3 such associations have been observed. Here it was assumed that the K^+ was produced with about the same cross-section as the θ^o_{anom} and that the K^+ and θ^o_{anom} lifetimes are about the same. The result of this examination predicted only 0.8 associations. Thus, the total predicted number of θ^o_{anom} associations for group A is not more than about two, which is not in serious disagreement with the total absence of any observed associations.

Using the technique discussed above, it is not possible to predict reliably how many θ^o_{anom} associations should be expected in group B, since the available statistics are much too poor. It is of some interest, however, to note that the (θ^o_{anom}, K^+) and $(\theta^o_{\pi 2}, K^+)$ associations have nearly the same detection probability, indicating (on the basis of very poor statistics!) that comparable numbers of these associations might be expected.

Although it is not possible to explain the associations quite perfectly on the basis of lifetime biases alone, the result of the preceding investigation does not mean that the discrepancy in observed associations cannot be entirely due to a lifetime bias. Unfortunately, the available number of θ^o_{anom} associations is too small at this time to make any

definite conclusions.

It is interesting to note that a crude description of the observations can also be made solely by assigning the θ^o_{anom} and $\theta^o_{\pi 2}$ particles strangeness quantum numbers of S = -1 and S = +1, respectively. This accounts for the presence of ($\theta^o_{\pi 2}$, hyperon) associations, and the corresponding absence of (θ^o_{anom}, hyperon) pairs. It accounts for the (θ^o_{anom}, $\theta^o_{\pi 2}$)association, and the absence of ($\theta^o_{\pi 2}$, $\theta^o_{\pi 2}$). Only the ($\theta^o_{\pi 2}$, K^+) observation seems to be in disagreement, but this could be explained by a case of (Ξ^-, $\theta^o_{\pi 2}$, K^+) or (Ξ^o, $\theta^o_{\pi 2}$, K^+) production, where the Ξ particle passes undetected.* In addition, there is further evidence from emulsion work[24] that several particles all having S = -1 are produced by interaction of θ^o_{anom} particles in emulsions. However, it may be that such particles are much more easily produced in emissions than, for example, K^+ particles.

Since there is no known theoretical basis for the description just discussed, while most of the features of the θ^o_{anom} particle seem to agree well with the theory of Gell-Mann and Pais, it would be rather surprising if the former description were correct. However, this description may be tested by using cloud chambers or bubble chambers in conjunction with the large accelerators to search for the charge exchange reactions:

---

* See figure 12 for classification of Ξ particle.

$$K^- + P \longrightarrow \overline{K^0} + N, \qquad \overline{K^0} \longrightarrow \theta^0_{\pi 2} \text{ decay} \qquad (36)$$

$$K^+ + N \longrightarrow K^0 + P, \qquad K^0 \longrightarrow \theta^0_{anom} \text{ decay} \qquad (37)$$

These reactions should be forbidden if the $\theta^0_{\pi 2}$ and θ^0_{anom} particles have S = +1, and S = -1, respectively. In fact, the reaction 36 now appears to have been confirmed by the Berkeley bubble chamber group.[25] Moreover, additional evidence has recently been provided[25] by the observation of K^+ particles produced in emulsions exposed to a beam of θ^0_{anom} particles; this reaction is the inverse of reaction 37. These results rule out the present conjecture.

VIII. CONCLUSIONS

The above analysis of 18 θ^{o}_{anom} decay events indicates that these involve 3 or more secondary particles, and probably arise from a K^{o} meson having approximately the mass of presently established K particles. Most of the decays cannot be explained by the scheme $\tau^{o} \rightarrow \pi^{+} + \pi^{-} + \pi^{o}$. However, all are consistent with the schemes $\theta^{o}_{anom} \longrightarrow \pi^{+} + \pi^{-} + \gamma$ and $\theta^{o}_{anom} \longrightarrow \pi^{\pm} + \mu^{\mp} + \nu$, with the exception of one decay having an identified electron secondary. All the decays are also consistent with the scheme $\theta^{o}_{anom} \longrightarrow \pi^{\pm} + e^{\mp} + \nu$, with the exception of one which has two identified L-meson secondaries. The θ^{o}_{anom} events cannot be entirely explained by merely a combination of τ^{o} decays and alternate decay modes of the $\theta^{o}_{\pi 2}$ particle.

From the distribution of the decays in the chamber, the lifetime of the θ^{o}_{anom} particle is found to be longer than that of the $\theta^{o}_{\pi 2}$ particles. There are also observed differences in momentum distributions and origin locations for the θ^{o}_{anom} and $\theta^{o}_{\pi 2}$ particles, and a large disparity exists between the fractions of each type of particle found traveling upward in the cloud chamber. However, a θ^{o}_{anom}-particle lifetime much longer than the lifetime of the $\theta^{o}_{\pi 2}$ particle can readily explain all these differences. The existence of the θ^{o}_{1} and θ^{o}_{2} particles proposed by Gell-Mann and Pais is in accord with these observed results. However, there is also found to be a considerable difference between the

types of particles observed in association with the θ^o_{anom} and $\theta^o_{\pi_2}$ particles. An examination was made of the possible effect of a strong lifetime bias upon the observed associations. Although the explanation of the observed associations by purely a lifetime bias is not entirely satisfactory, there is no strong evidence against this explanation. It is felt that further experimental work needs to be done to clarify the matter of θ^o_{anom} vs. $\theta^o_{\pi_2}$ associations.

Assuming that θ^o_{anom} decays arise from the θ^o_2 particle and $\theta^o_{\pi_2}$ decays from the θ^o_1 particle, a lower limit to the θ^o_2 lifetime is found from the relative number of observed decays to be $0.7_{-0.33} \times 10^{-8}$ sec.

REFERENCES

1. Proceedings of Third Annual Rochester Conference, December, 1952, University of Rochester.
2. Van Lint, Anderson, Cowan, Leighton, and York, Phys. Rev. 94, 1732 (1954).
3. R. W. Thompson, et al. Phys. Rev. 90, 329 (1953). R. W. Huggett, J. R. Burwell, and R. W. Thompson, Phys. Rev. 98, 248 (1955). Fourth Rochester Conference on High Energy Physics, 1954 (Univ. of Roch. Press).
4. W. H. Arnold, Jr., W. Martin, and H. W. Wyld, Phys. Rev. 100, 1545 (1955). J. Ballam, M. Grisaru, and S. B. Treiman, Phys. Rev. 101, 1438 (1956).
5. Progress in Cosmic Ray Physics, vol. III.
6. M. Gell-Mann and A. Pais, Phys. Rev. 97, 1387 (1955).
7. J. A. Kadyk, G. H. Trilling, R. B. Leighton, and C. D. Anderson, Bull. Amer. Phys. Soc. 1, 251 (1956).
8. J. P. Astbury, Nuovo Cimento 12, 387 (1954).
9. R. Armenteros, K. H. Barker, C. C. Butler, and A. Cachon, Phil. Mag. 42, 1113 (1951).
10. R. B. Leighton, S. D. Wanless, and C. D. Anderson, Phys. Rev. 89, 148 (1953).
11. V. A. J. van Lint, Ph.D. Thesis, California Institute of Technology, 1954 (unpublished).
12. R. B. Leighton, Rev. Sci. Inst., 27, 79 (1956).
13. Bethe, Phys. Rev. 70, 821 (1946).

14. G. Yekutieli, M. F. Kaplon, and T. F. Loang, Phys. Rev. 101, 506 (1956); Phys. Rev. 101, 1834 (1956).

15. S. B. Treiman, Phys. Rev. 75, 1360 (1954).

16. K. Lande, E. T. Booth, J. Impeduglia, and L. M. Lederman, Phys. Rev. 103, 1901 (1956).

17. Arnold A. Strassenburg, Ph.D. Thesis, California Institute of Technology, 1955.

18. M. S. Bartlett, Phil. Mag. 44, 249 (1953).

19. G. H. Trilling and R. B. Leighton, Phys. Rev. 104, 1703 (1951).

20. J. E. Osher, Ph.D. Thesis 1956, Univ. of Calif. Rad. Lab.

21. J. Ballam, D. R. Harris, A. L. Hodson, R. Ronald Rou, G. T. Reynolds, S. B. Treiman and M. Vidale, Phys. Rev. 91, 1019 (1954); G. T. Reynolds and S. B. Treiman, Phys. Rev. 94, 207.

22. W. B. Fowler, R. P. Shutt, A. M. Thorndike and W. L. Whittemore, Phys. Rev. 93, 861 (1954); Phys. Rev. 98, 121 (1955).

23. R. Budde, M. Chretien, J. Leitner, N. P. Samios, M. Schwartz, and J. Steinberger, Phys. Rev. 103, 1827 (1956).

24. W. F. Fry, J. Schneps, and M. S. Swami, Phys. Rev. 103, 1904 (1956).

25. Robert D. Tripp, Radiation Laboratory of University of California, and Dr. M. Gell-Mann (private communications).

APPENDIX A

MOMENTUM MEASUREMENT AND ASSIGNMENT OF MOMENTUM ERRORS

1. Anisotropic Projector

The photograph of the cloud chamber track is reprojected by the anisotropic projector,[12] and the image is traced on paper at least 3 times for subsequent measurement. The projector magnifies the photograph image by 5 in the longitudinal direction (along chord of track), and by 50 in the transverse direction.

2. Notation

Symbols defined on pp. 5 and 6 are used. A prime mark attached to one of these symbols, e.g. S', indicates the quantity as measured from the image formed by the projector. Since the magnification of the photographic system is 1/9, the following relations exist between primed and unprimed quantities:

$$S' \frac{50}{9} S \qquad L' \frac{5}{9} L \tag{38}$$

3. Momentum Measurement

The apparent radius of curvature of the track, uncorrected for conical projection or dip, is given by

$$\rho_a = \frac{L^2}{8S} + \frac{S}{2} \simeq \frac{L^2}{8S} \tag{39}$$

where the approximation is valid for all tracks much above

100 Mev/c. ρ_a is found directly from the tracings by combining equations 38 and 39:

$$\rho_a = \left(\frac{9L'}{5}\right)^2 \frac{1}{8\left(\frac{9S'}{50}\right)} + \frac{1}{2}\frac{9}{50}S' = \frac{9}{4}\frac{L'^2}{S'} + \frac{9S'}{100} \simeq \frac{9L'^2}{4S'} \quad (40)$$

The momentum is found by applying suitable corrections[11] to the formula

$$P(\text{Mev/c}) = 3B\rho_a \quad (41)$$

where B is in MKS units, and ρa in cm.

4. Measurement Error

The error incurred in the measurement process arises from inaccuracies in tracing the track, and especially from the uncertainty in the location of the center of the track, to which S' is measured. The projected track image is typically 5 mm. wide at its midpoint. It was found that one standard deviation in measurement error is approximately equivalent to an assigned error in S' of

$$S'_M = 0.1 \text{ cm.}$$

The relative measurement error is then

$$e_M = \frac{S'_M}{S'} = \frac{0.1}{S'} = \frac{10}{S'} \ (\%) \quad (42)$$

5. Distortion Error

The distortion error is obtained by assuming an un-

certainty, S_D', in the measured sagitta, S', corresponding to the observed maximum detectable momentum, p_{max}, which is observed to be about 3,300 Mev/c for a 20 cm track. As discussed in section II.C.2, S_D' is taken to be proportional to L', and by equation 7 of that section, using $B \simeq 0.8$ webers/m^2, p_{max} is approximately

$$p_{max} \simeq 2.4 \frac{L^2}{8 S_D}$$

Normalizing to a 20 cm track, and using equation 38

$$3300 \simeq 2.4 \frac{(20)^2}{8 S_{D_0}}, \quad S_{D_0} = 0.036 \text{ cm},$$

$$S_{D_0}' = \frac{50}{9}(0.036) = 0.20 \text{ cm},$$

$$S_D' = S_{D_0}'\left(\frac{L}{20}\right) = 0.20\left(\frac{L}{20}\right)$$

The relative distortion error is then, by equations 38 and 40,

$$e_D = \frac{S_D'}{S'} \simeq 0.20\left(\frac{L}{20}\right)\frac{p_a}{\frac{3}{4}L'^2} = 0.008\frac{p_a}{L'}$$

$$e_D = 0.8\frac{p_a}{L'}\ (\%) \qquad (43)$$

6. Scattering Error

The relation for scattering error is based upon work of Bethe,[13]

$$\frac{|\Delta\rho|}{\rho} = 16.5 \times 10^{-4}\frac{Z_1}{B\beta}\sqrt{\frac{2NA}{L}} \qquad (44)$$

where Z = atomic number of absorber,

N = moles/cm^3 of absorber,

A = near unity, and slowly varying.

If $\frac{\Delta\rho}{\rho}$ is less than about 10%, as is usually the case, then

$$e_s = \frac{S_s}{S} = \frac{\left|\Delta\left(\frac{1}{\rho}\right)\right|}{\frac{1}{\rho}} \simeq \frac{\Delta\rho}{\rho} \qquad (45)$$

7. Total Error

All three errors are assumed to be independent, and the total relative error in the sagitta is:

$$e = \sqrt{e_M^2 + e_D^2 + e_S^2}$$

Since the momentum is inversely proportional to S, the momentum errors are asymmetric, and given by

$$\Delta p = \frac{p}{\left(\frac{1}{e}\right) \mp 1}$$

APPENDIX B

P* vs Q(1,2)

For a three-body decay into charged particles 1 and 2, and neutral particle 3, from a parent particle of mass M_o, the following relations are true:

$$\underline{P}_1^* + \underline{P}_2^* + \underline{P}_3^* = 0, \quad \underline{P}_1 + \underline{P}_2 + \underline{P}_3 = \underline{P}_o \tag{46}$$

$$E_1^* + E_2^* + E_3^* = M_o, \quad E_1 + E_2 + E_3 = E_o \tag{47}$$

The calculated Q value on the basis of a two-body decay is related to equations 46 and 47 by

$$(E_1 + E_2)^2 - (\underline{P}_1 + \underline{P}_2)^2 = \left[Q(1,2) + m_1 + m_2\right] = M^2$$

where M is the apparent mass of the parent particle, based upon the assumption of a two-body decay. As a result of relativistic invariance,

$$(E_1 + E_2)^2 - (\underline{P}_1 + \underline{P}_2)^2 = (E_1^* + E_2^*)^2 - (\underline{P}_1^* + \underline{P}_2^*)^2,$$

$$\underline{P}_1^* + \underline{P}_2^* = \underline{P}^* = -\underline{P}_3^* \tag{48}$$

From equations 47 and 48:

$$\sqrt{M^2 + (P^*)^2} + \sqrt{m_3^2 + (P^*)^2} = M_o$$

Solving for P* in terms of Q(1,2):

$$M^2 + (P^*)^2 = M_o^2 - 2M_o\sqrt{m_3^2 + (P^*)^2} + m_3^2 + (P^*)^2$$

$$4M_o^2\left[m_3^2 + (P^*)^2\right] = \left[M_o^2 + m_3^2 - M^2\right]^2$$

$$P^* = \sqrt{\left[\frac{M_o^2 + m_3^2 - M^2}{2M_o}\right]^2 - m_3^2} = \sqrt{\left\{\frac{M_o^2 + m_3^2 - \left[Q(1,2) + m_1 + m_2\right]^2}{2M_o}\right\}^2 - m_3^2} \qquad (49)$$

If $m_3 = 0$, as in decays B, C, and D of part IV, then equation 48 simplifies to

$$P^* = \frac{M_o^2 - \left[Q(1,2) + m_1 + m_2\right]^2}{2M_o} \qquad (50)$$

Relations 49 and 50 have been used in plotting the curves in figures 6-8.

APPENDIX C

Formula for $\gamma\beta$

Several different forms of the relation for $\gamma\beta$ may be derived, involving P_L, P_L^*, E, and E* in different ways. However, the most useful relation appears to be the following, derived from the Lorentz transformations:

$$P_L = \gamma P_L^* + \gamma\beta E^*, \quad E = \gamma E^* + \gamma\beta P_L^*$$

Eliminating γ :

$$\frac{P_L^*}{E^*} \quad \frac{\gamma\beta E^* - P_L}{\gamma\beta P_L^* - E}, \quad \gamma\beta\left[(E^*)^2 - (P_L^*)^2\right] = E^* P_L - E P_L^*$$

$$\gamma\beta = \frac{E^* P_L - E P_L^*}{(E^*)^2 - (P_L^*)^2} = \frac{E^* P_L - E P_L^*}{M^2 + P_\perp^2} \tag{51}$$

where $E^* = \sqrt{(P^*)^2 + M^2}$, $E = \sqrt{P^2 + M^2}$, and M and P* are found from Q(1,2) (see Appendix C). In the calculation of $\gamma\beta$, various special circumstances may arise:

1. The Origin is Observed

In this case, P_L and $P_\perp$ may be determined, but the sign of

$$P_L^* = \pm\sqrt{(P^*)^2 - P_\perp^2} \tag{52}$$

is ambiguous and there are, in general, two corresponding values of $\gamma\beta$, which are called $\gamma\beta_{min}$ and $\gamma\beta_{max}$. How-

ever, if $P < P^*$, then the lower sign in equation 52 must be taken, and $\gamma\beta$ is uniquely determined.

2. The Origin is Not Observed

Only upper and lower limits on $\gamma\beta$ can be set in this case. $\gamma\beta_{max}$ is determined by assuming $P_L^* = -P^*$; $\gamma\beta_{min}$ is most easily found by trial of various values of $P_\perp$ in the equations:

$$\gamma\beta_{min} = \frac{-E^*\sqrt{P^2 - P_\perp^2} + E\sqrt{(P^*)^2 - P_\perp^2}}{M^2 + P_\perp^2}, \quad P < P^*$$

$$\gamma\beta_{min} = \frac{E^*\sqrt{P^2 - P_\perp^2} - E\sqrt{(P^*)^2 - P_\perp^2}}{M^2 + P_\perp^2}, \quad P > P^*$$

APPENDIX D

DECAY DYNAMICS

1. Estimate of P_o for $\theta_{\pi 2}$ Decay

In many $\theta^o_{\pi 2}$ decay events in which one or both secondary momenta are unmeasurable, it is nevertheless possible to estimate the momentum of the $\theta^o_{\pi 2}$ particle fairly closely by measuring only θ. This is because of the symmetric nature of the two-body decay. Since both secondaries have equal masses, the angle θ tends to be independent of the decay orientation for a wide range of θ^*, and depends primarily upon $\gamma\beta = \frac{P_o}{M_o}$. This can be seen as follows:

Define: p_{1L}, p_{2L} = longitudinal component of momenta of secondary particles in laboratory system.

p^* = momentum of secondary particles in C.M. system.

e^* = energy of secondaries in C.M. system.

θ_1, θ_2 = angles made by secondaries with L.O.F. of $\theta^o_{\pi 2}$.

θ^* = angle of emission in C.M. system of particle 1.

$$p_{1L} = \gamma p^* \cos\theta^* + \gamma\beta e^*, \quad p_{2L} = -\gamma p^* \cos\theta^* + \gamma\beta e^*$$

$$\tan\theta_1 = \frac{p^* \sin\theta^*}{\gamma p^* \cos\theta^* + \gamma\beta e^*}, \quad \tan\theta_2 = \frac{p^* \sin\theta^*}{-\gamma p^* \cos\theta^* + \gamma\beta e^*}$$

$$\tan\theta = \tan(\theta_1 + \theta_2) = \frac{2\gamma\beta e^* p^* \sin\theta^*}{(\gamma\beta e^*)^2 - (\gamma p^* \cos\theta^*)^2 - (p^* \sin\theta^*)^2}$$

Let: $a = \frac{e^*}{p^*} = \frac{247}{204} = 1.215$

$b = \gamma\beta$

then:

$$\tan\theta = \frac{2ab\sin\theta^*}{a^2b^2 - 1 - b^2\cos^2\theta^*}$$

Since the probability of decay is proportional to $\sin\theta^*$, most decays will have $\theta^* \sim 90^\circ$. However, $\tan\theta$ is approximately constant for any θ^* near 90°:

$$\frac{\partial(\tan\theta)}{\partial\theta^*} = \frac{2ab\cos\theta^*\left[a^2b^2 - 1 - b^2(1+\sin^2\theta^*)\right]}{(a^2b^2 - 1 - b^2\cos^2\theta^*)^2}$$

$$\left.\frac{\partial(\tan\theta)}{\partial\theta^*}\right|_{\theta^*=90^\circ} = 0$$

As an example, figure 13 shows θ plotted vs. θ^* for $\gamma\beta = 2$, or $P_o \simeq 1000$ Mev/c; many $\theta^o_{\pi 2}$ particles have momenta of about this value. For $\gamma\beta = 2$, over 90% of the decays occur with $\tan\theta$ within 20% of the mean value, $\langle\tan\theta\rangle$:

$$\langle\tan\theta\rangle = \frac{a\pi}{b}\left(1 - \sqrt{1 - \frac{b^2}{a^2b^2 - 1}}\right) \approx \frac{800}{P_o}, \quad P_o > 700 \text{ Mev/c}$$

or

$$P_o \approx \frac{800}{\langle\tan\theta\rangle}$$

For nearly all decays, then

$$P_o \approx \frac{800}{\tan\theta}$$

An upper limit on P_o is given by this relation in the few

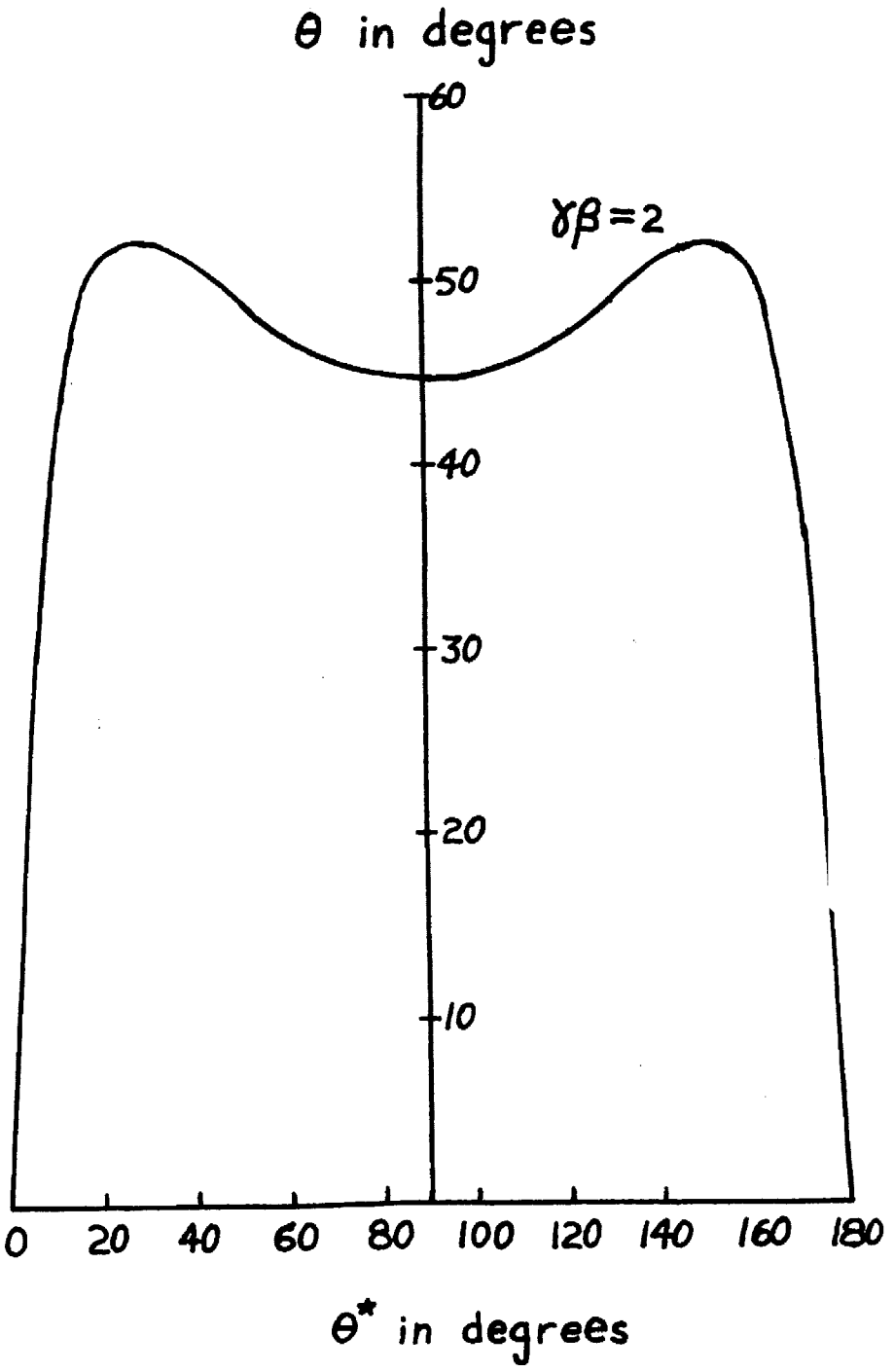
θ in degrees
60
50
40
30
20
10
γβ=2
0
20
40
60
80
100
120
140
160
180
θ* in degrees

Figure 13

cases where $|\theta^*| \lesssim 15^\circ$; when this happens, it is usually apparent from the difference in the observed momenta of the secondaries that the estimate is no longer valid. For θ°_{anom} decays where $Q(\pi^+, \pi^-) < 65$ Mev, $p^* \leqslant 100$, and

$$P_o\,(\text{Mev/c}) \lesssim \frac{400}{\tan\theta}$$

2. Q value Distribution for $\theta^\circ_{anom} \longrightarrow \pi^\pm + \mu^\mp + \nu$

In the absence of any detailed knowledge concerning the angular dependence of the decay, it is assumed that the decay distributions depend upon statistical factors alone. The Q-value distribution depends only upon the distribution in energy of the neutral secondary,[11] since:

$$Q(1,2) = \sqrt{(M_o - m_3)^2 - 2M_o T_3^*} - (m_1 + m_2)$$

where T_3^* = kinetic energy of neutral secondary in C.M. system, or for the decay $\theta^\circ_{anom} \longrightarrow \pi^\pm + \mu^\mp + \nu$,

$$Q(1,2) = \sqrt{M_o^2 - 2M_o P_3^*} - (m_1 + m_2)$$

The distribution of P_3^* is known for a three-body decay,[11] and is used to plot the distribution for Q(1,2) shown in figure 14. From this distribution, it is found that about 1/3 of the decays occur with a value of $Q < 65$ Mev.

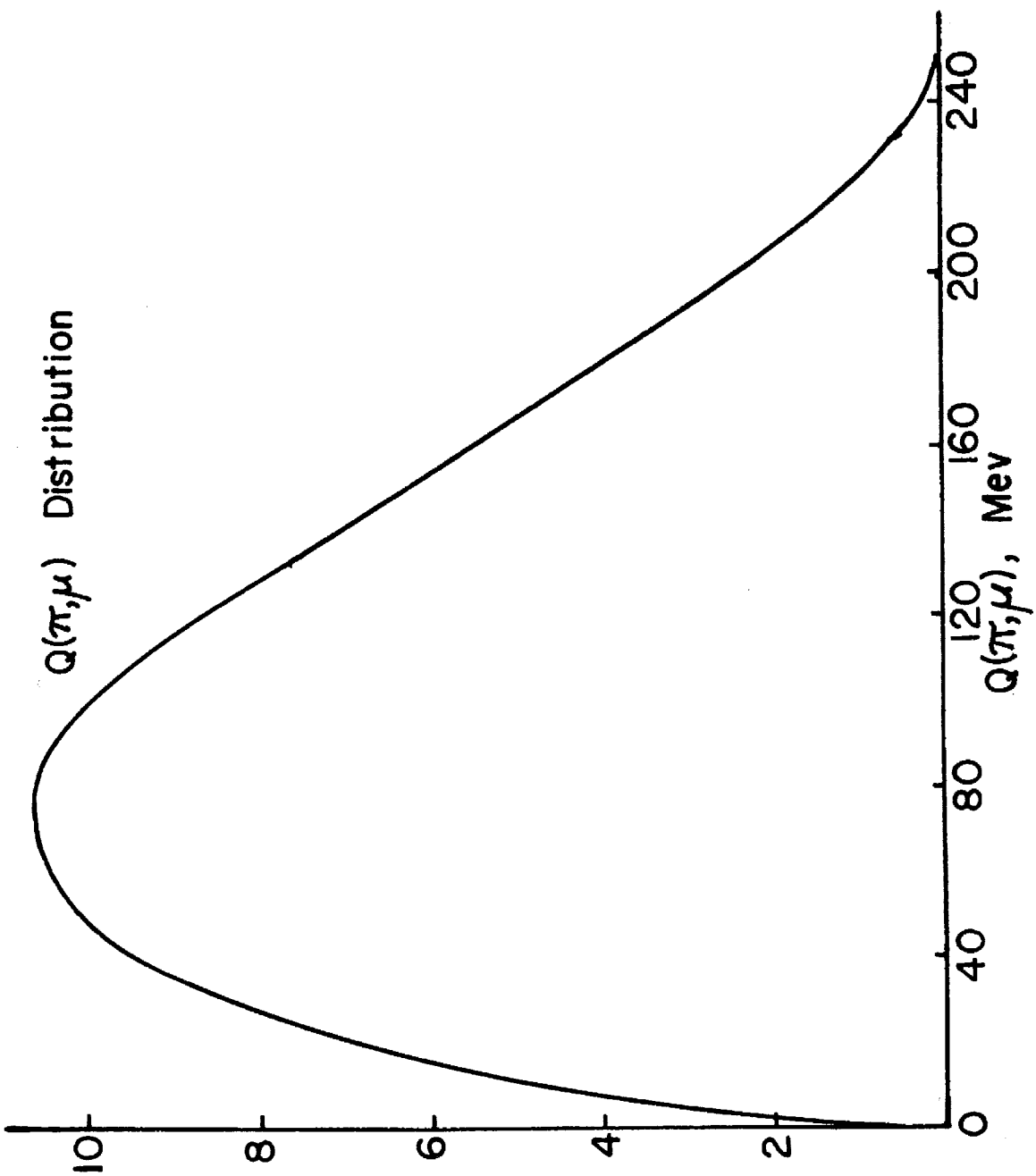

Figure 14